Eleventh International Conference on Computational Fluid Dynamics (ICCFD11), Maui, Hawaii, USA, July 11-15, 2022

ICCFD11-2022-1003

Discontinuous Galerkin and Related Methods for ODE

H. T. Huynh
huynh@grc.nasa.gov
NASA Glenn Research Center, MS 5-11,
Cleveland, OH 44135, USA.

Abstract: A defining feature of the discontinuous Galerkin (DG) method for ODE is that the piecewise polynomial solution can have a jump discontinuity at the beginning of each step. Starting from the standard integral formulation, the DG method is derived here in differential form. The key ingredient is a polynomial called the correction function, which helps 'correct' the discontinuous solution by approximating the jump and yields a continuous one. Under the right Radau quadrature, this continuous solution is identical to the solutions by the right Radau collocation and the continuous Galerkin (CG) methods. Next, the correction function facilitates the construction of the associated implicit Runge-Kutta schemes (IRK-DG). Different quadratures for DG result in different IRK-DG methods: left Radau quadrature in Radau IA, right Radau quadrature in Radau IIA or right Radau collocation, and Gauss quadrature in a method called DG-Gauss. The construction of IRK-DG clarifies the meaning and facilitates the proofs of various $B(p)$, $C(\eta)$, and $D(\zeta)$ conditions for accuracy. The two consequences of these conditions are that all s-stage IRK-DG methods are accurate to order $2s-1$, and the IRK-DG methods of Radau type are unique. Numerical examples showing the behavior of the DG solutions are provided. In all, the correction function plays a key role and helps establish the relations among the DG, IRK-DG, collocation, and CG schemes.

Keywords: Discontinuous Galerkin, implicit Runge-Kutta, collocation, continuous Galerkin, time stepping, numerical methods, ordinary differential equations.

1 Introduction

The finite element method is popular for numerically solving partial differential equations as well as ordinary differential equations (e.g., Eriksson et al. 1996, Johnson 2012, Hughes 2012). The continuous finite element, or continuous Galerkin (CG), method was first employed to solve ODE by Argyris & Scharpf (1969) and Fried (1969). Hulme (1972) showed that the CG method for ODE is equivalent to the collocation method using quadrature points as collocation points.

Collocation is an idea widely applicable in numerical analysis. For ODE, collocation methods enforce the differential equation at the collocation points. These methods were studied by Cooper (1968) and Axelsson (1969). Wright (1970) showed that the collocation process leads to an implicit Runge-Kutta (IRK) scheme. Collocation methods are covered in most texts on numerical methods for ODE (e.g., Hairer, Norsett, & Wanner 1993, Hairer & Wanner 1991, Lambert 1991).

The discontinuous Galerkin (DG) method, which allows jump discontinuities across cells or elements, was introduced by Reed & Hill (1973) for the neutron transport equation. These methods are popular for the spatial discretization of conservation laws (Cockburn, Karniadakis, & Shu 2000). LeSaint & Raviart (1974) formulated the DG method for ODE and showed, by employing the left Radau quadrature, that the method results in an IRK scheme that is A-stable and superconvergent. Delfour, Hager, & Trochu (1981) generalized the DG method by using a weighted average of the left and right values for the boundary terms

of each step and proved the superconvergence property of the resulting method. In general, such a weighted average leads to the coupling among the steps and a very large system of equations, and the method is no longer of one-step type. More recent efforts on unifying frameworks for DG and related methods as well as their associated IRK schemes include the contributions of Borri & Bottasso (1993), Bottasso (1997), Tang & Sun (2012), and Zhao & Wei (2014). Dissipative dynamical behavior of the DG method was studied by Estep & Stuart (2001). A posteriori error estimates of the DG method was explored by Baccouch (2016). A time finite element method based on Hamilton's variational principle can be found in Xing, Qiu, & Guo (2017). An adaptive DG method for very stiff systems was investigated by Fortina & Yakoubi (2019). Additional contributions can be found in the cited references. A common feature of papers on this subject is that they are typically highly algebraic and/or analytic, centering on error estimates and stability analyses.

In this paper, we study the DG method for ODE from a perspective different from those in the literature. Our focus is on constructing the solution. This task is accomplished by removing the test function in the integral formulation and deriving the DG method in differential form. The key ingredient is a polynomial called the correction function, which helps 'correct' the discontinuous solution by approximating the jump at the beginning of each step. The result is a continuous solution for the DG method. Under the right Radau quadrature, this continuous solution is identical to the solutions by the right Radau collocation and the CG methods. Next, the correction function facilitates the construction of the associated implicit Runge-Kutta schemes (IRK-DG). Different quadratures for DG result in different IRK-DG methods: left Radau quadrature in Radau IA, right Radau quadrature in Radau IIA or right Radau collocation, and Gauss quadrature in a method called DG-Gauss. All s-stage IRK-DG methods are shown to be accurate to order $2s-1$. The proof is carried out by employing the IRK-DG construction to derive various $B(p)$, $C(\eta)$, and $D(\zeta)$ conditions. The $C(s)$ and $D(s)$ conditions also lead to uniqueness of the Radau type methods. Numerical examples showing the behavior of the DG solutions are provided. In sum, the correction function plays a crucial role and helps clarify the relations among the DG and related schemes.

This paper is essentially self-contained and organized as follows: the DG method is presented in §2, the resulting IRK-DG §3, accuracy §4, numerical examples §5, and conclusions and discussion §6.

2 Discontinuous Galerkin (DG) Formulation for ODE

For simplicity and with no loss of generality, instead of a system of equations, consider a scalar ODE:

$$u'(x) = f\big(x, u(x)\big)$$

with initial condition

$$u(x_0) = u_0.$$

Assuming a solution exists, the methods studied are of one-step type: the data u_n at x_n is known and, with step size h (may depend on n), the solution u_{n+1} at $x_{n+1} = x_n + h$ is to be calculated, $n = 0, 1, 2, \ldots$.

The DG method approximates the solution on $(x_n, x_n + h]$ by a polynomial u_h of degree k. At each x_n, the data is $u_n = u_h(x_n^-)$, i.e., upwinding is employed; for $n = 0$, the data is the initial condition u_0. A defining feature of the method is that the piecewise polynomial function u_h can be and usually is discontinuous across each x_n, i.e., $u_h(x_n^-) \neq u_h(x_n^+)$. The solution is $u_{n+1} = u_h(x_{n+1}^-)$.

As is routine, the reference or local variable ξ on $[0, 1]$ is employed:

$$x = x_n + \xi h.$$

A function $v(x)$ on $[x_n, x_{n+1}]$ corresponds to a function on $[0, 1]$ also denoted by v: $v(\xi) = v(x(\xi))$. By applying the chain rule to the ODE,

$$\frac{du}{d\xi} = hf\big(\xi, u(\xi)\big).$$

For the moment, with no loss of generality, we assume

$$h = 1.$$

Loosely put, h is absorbed into f. The case of a general h is straightforward and will be expressed later.

In the rest of this paper, we employ the notation

$$u' = \frac{du}{d\xi}.$$

Thus, using the local coordinate ξ with the assumption $h = 1$, the ODE takes the form: on $[0, 1]$,

$$u'(\xi) = f\big(\xi, u(\xi)\big), \qquad u(0) = u_n. \tag{2.1}$$

Denote by $\boldsymbol{P}_k$ the space of polynomials of degree k or less, by $\mathcal{P}_k$ the projection onto $\boldsymbol{P}_k$ and, for any two functions v and w on $[0, 1]$ (usually polynomials here),

$$(v, w) = \int_0^1 v(\xi) w(\xi) d\xi.$$

To solve $u'(\xi) = f(\xi, u(\xi))$, the DG method seeks a polynomial u_h of degree k on $(0, 1]$, such that for any v in $\boldsymbol{P}_k$, (u_h', v) nearly equals (f, v); the precise criteria is given by (2.3) below. To involve u_n, by integration by parts,

$$(u_h', v) = u_h(1)v(1) - u_h(0^+)v(0) - (u_h, v').$$

At $\xi = 0$, the data u_n is more critical and is employed instead of $u_h(0^+)$ above.

The DG method seeks u_h of degree k on $(0, 1]$ such that for any v in $\boldsymbol{P}_k$ (called a test function),

$$u_h(1)v(1) - u_n v(0) - (u_h, v') = (f, v). \tag{2.2}$$

The above is often called the weak form. Integrate (u_h, v') by parts, we obtain the strong form

$$[u_h(0^+) - u_n]v(0) + (u_h', v) = (f, v). \tag{2.3}$$

At x_{n+1}, the solution u_{n+1} is, in the local coordinate,

$$u_{n+1} = u_h(1) = u_h(1^-). \tag{2.4}$$

Strictly speaking, u_h is defined on (0,1]. To simplify the notation, its domain is extended to [0,1] by

$$u_h(0) = u_h(0^+).$$

Since $v \in \boldsymbol{P}_k$, we can replace f on the right-hand side of (2.3) by its projection onto $\boldsymbol{P}_k$, i.e., $\mathcal{P}_k(f)$. Set

$$f_h = \mathcal{P}_k(f). \tag{2.5}$$

By the above two equations, the strong form (2.3) can be written as

$$[u_h(0) - u_n]v(0) + (u_h', v) = (f_h, v). \tag{2.6}$$

Note that $f_h = \mathcal{P}_k(f)$ is of degree k, and u_h', degree $k - 1$. Loosely put, u_h' nearly equals f_h except for the term $[u_h(0) - u_n]v(0)$.

The following simple example shows the essential properties of the DG solution. With ξ on $[0, 1]$, solve

$$u'(\xi) = f(\xi) = 6\xi - 5, \qquad u(0) = 3.$$

The exact solution is trivial,

$$U(\xi) = 3\xi^2 - 5\xi + 3. \tag{2.7}$$

For the linear DG solution $u_h(\xi) = a\xi + b$, on $[0, 1]$, by the strong form (2.6) with $v = 1$ and $v = \xi$, a little algebra yields $a = -1$ and $b = 2$, or

$$u_h(\xi) = -\xi + 2. \tag{2.8}$$

The solution at the end of the step is $u_h(1) = U(1) = 1$. (See Fig. 2.1.)

Next, on $[0, 1]$, the two left Radau points are 0 and $2/3$, and right Radau points, $1/3$ and 1. The quadratic solution U of (2.7) and the linear DG solution u_h above intersect at $(1/3,\ 5/3)$ and $(1,1)$ i.e., the abscissas of their intersections are the two right Radau points (see Fig. 2.1b). Whereas U satisfies $U(0) = u_n = 3$, the DG solution u_h does not, and u_h interpolates U at the two right Radau points and is defined by the values of U at these two points. On the other hand, u_h' and U' intersect at $(2/3, -1)$, i.e., the abscissa of their intersection is the interior left Radau point (see Fig. 2.1a). That is, the solutions U and u_h match at the right Radau points, and their derivatives U' and u_h' match at the interior left Radau points.

It will be shown that (a) the above relation for U and u_h as well as that for U' and u_h' hold true for the general case; (b) the left and right Radau points also play an essential role in the approximate Dirac delta and the correction functions, respectively; and (c) U is a collocation as well as a CG solution.

Fig. 2.1a shows the plots of $f(\xi) = 6\xi - 5$ (thick blue line) and $u_h' = -1$ (dot-dashed green line); the ξ-coordinate of their intersection is the nonzero member of the two left Radau points (blue square dots on ξ-axis). Fig. 2.1b shows the (exact) quadratic solution U (thick blue curve) and the linear DG solution u_h (dot-dashed green line); the intersections of U and u_h (big red round dots) and their ξ-coordinates, which are the two right Radau points (small red round dots).

We can also turn the problem around and ask: on $[0, 1]$, how do we evaluate the derivative of the discontinuous function u_h defined by $u_h(0) = 3$ and, for $0 < \xi \le 1$, $u_h(\xi) = -\xi + 2$? The answer is that the DG method amounts to the following derivative evaluation: reconstruct the solution via U of one degree higher than u_h that interpolates u_h at the right Radau points and satisfies $U(0) = 3$: $U = 3\xi^2 - 5\xi + 3$; the derivative of the discontinuous function u_h is given by U'. Note that U' is of the same degree as u_h. Such a derivative estimate for a polynomial with a jump discontinuity also holds true for the general case.

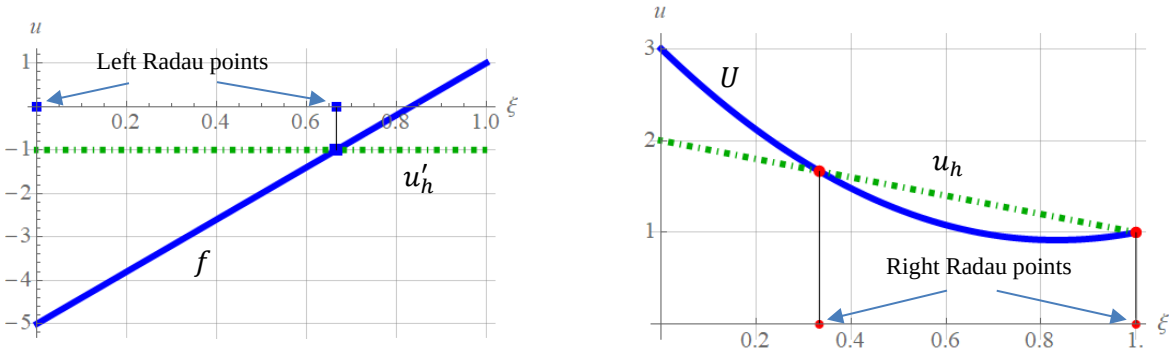

(**a**) (**b**)

Fig. 2.1 The graphs of (**a**) $f(\xi) = 6\xi - 5$ (thick blue line), $u_h' = -1$ (dot-dashed green line), and the two left Radau points (blue square dots on ξ-axis); and (**b**) the quadratic solution U (thick blue curve), the linear DG solution u_h (dot-dashed green line), and the two right Radau points (red round dots).

Approximate Dirac Delta Function γ at $\xi = 0$

The standard approach is to solve the weak form (2.2) or the strong form (2.3). Here, the goal is to define a polynomial U of degree $k + 1$ closely related to u_h and has the properties that

$$U' = f_h \quad \text{and} \quad U(0) = u_n. \tag{2.9}$$

In other words, we wish to eliminate the test function v in (2.6).

To this end, let $\mathbb{R}$ be the real line. The mapping B from $\boldsymbol{P}_k$ to $\mathbb{R}$ defined by, for each v in $\boldsymbol{P}_k$,

$$B(v) = v(0),$$

is a linear functional on $\boldsymbol{P}_k$. Thus, there exists γ in $\boldsymbol{P}_k$ such that $B(v) = (\gamma, v)$, i.e.,

$$(\gamma, v) = v(0). \tag{2.10}$$

The polynomial γ of degree k is called an approximate Dirac delta function for the following reason. In our context, on $[0, 1]$, let the Dirac delta function at $\xi = 0$ be denoted by δ_0 and defined by $\delta_0(v) = v(0)$ for any continuous function v on $[0, 1]$. Then γ defined above is an approximation of δ_0 by an element of $\boldsymbol{P}_k$.

In fact, γ can be expressed explicitly. Let the $k + 1$ left Radau points on $[0, 1]$ be denoted by $\xi_{L,1}$, …, $\xi_{L,k+1}$ where $\xi_{L,1} = 0$. Let $l_{L,1}$, …, $l_{L,k+1}$ be the corresponding Lagrange (basis) polynomials, which are of degree k and satisfy $l_{L,j}(\xi_{L,i}) = \delta_{i,j}$. Then

$$\gamma = (k+1)^2 l_{L,1}. \tag{2.11}$$

To show the above, let the corresponding left Radau quadrature weights be $b_{L,1}$, …, $b_{L,k+1}$ where

$$b_{L,1} = \frac{1}{(k+1)^2}. \tag{2.12}$$

(The standard weight of $2/(k+1)^2$ is due to the domain being $[-1, 1]$; see, e.g., Hildebrand 1974). Recall that the Radau quadrature with $k+1$ evaluation points has a degree of precision $2k$, i.e., it is exact for any polynomial of degree $2k$ or less. Consequently, for any v in $\boldsymbol{P}_k$, since $l_{L,1}v$ is of degree $2k$ or less, by applying the left Radau quadrature, and since $l_{L,1}$ vanishes at all Left Radau points except at $\xi_{L,1} = 0$,

$$(l_{L,1}, v) = \int_0^1 l_{L,1}(\xi) v(\xi) d\xi = b_{L,1} v(0) = \frac{1}{(k+1)^2} v(0).$$

That is,

$$\big((k+1)^2 l_{L,1}, v\big) = v(0).$$

The above and (2.10) completes the proof of (2.11).

Fig. 2.2a shows the 3 left Radau points (blue square dots on the ξ-axis) and the corresponding Lagrange polynomials for $k = 2$, and Fig. 2.2b shows the approximate Dirac delta function γ for $k = 8$ (thin blue curve) and $k = 9$ (red thick curve).

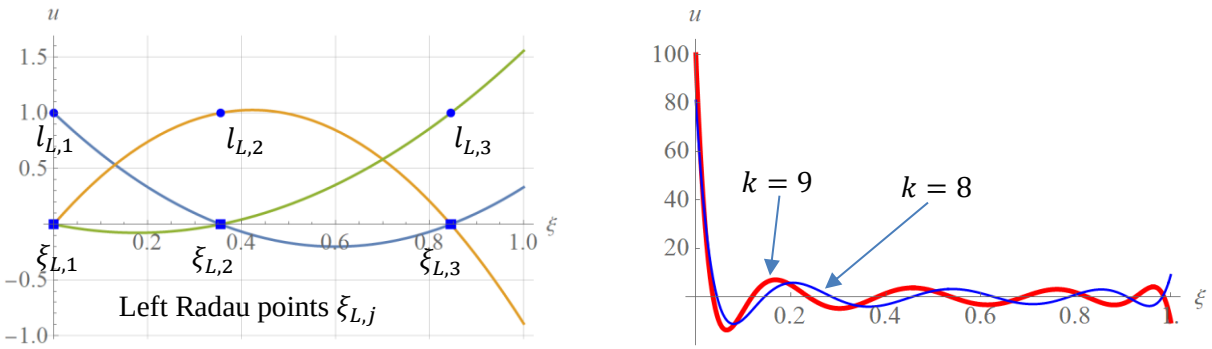

(a) **(b)**

Fig. 2.2 (a) The left Radau points $\xi_{L,j}$ (blue square dots) and the corresponding Lagrange polynomials $l_{L,j}$, $j = 1, 2, 3$ for $k = 2$. (**b**) The approximate Dirac delta function $\gamma = (k+1)^2 l_{L,1}$ for $k = 8$ (blue thin curve) and $k = 9$ (red thick curve).

With γ as in (2.11), by using (2.10), the strong form (2.6) can be written as

$$[u_h(0) - u_n](\gamma, v) + (u_h', v) = (f_h, v). \tag{2.13}$$

That is (recall $u_h' = du/d\xi$ and h is absorbed into f), on $[0, 1]$,

$$[u_h(0) - u_n]\gamma + u_h' = f_h. \tag{2.14}$$

Here, u_h' is of degree $k-1$, but γ is of degree k matching that of $f_h = \mathcal{P}_k(f)$.

It will be shown later that by using a quadrature for DG, f_h can be defined by its values at the quadrature points. As such, the above equation yields a differential formulation for DG involving no inner products.

The left Radau points play a special role in the above differential formulation. Indeed, by (2.11), the above implies

$$u_h' - [u_n - u_h(0)](k+1)^2 l_{L,1} = f_h. \tag{2.15}$$

Thus, in solving $u' = f$, the DG solution u_h satisfies, at the interior left Radau points $\xi_{L,j}$, i.e., for $2 \le j \le k+1$,

$$u_h'(\xi_{L,j}) = f_h(\xi_{L,j}) \tag{2.16}$$

and for $j = 1$, i.e., at $\xi = \xi_{L,1} = 0$, by (2.15),

$$u_h'(0) - (k+1)^2[u_n - u_h(0)] = f_h(0). \tag{2.17}$$

Loosely put, the jump in function values at $\xi = 0$ from u_n to $u_h(0)$ does not alter the derivative at the nonzero left Radau points by (2.16); however, at $\xi = 0$, by the above, the derivative $u_h'(0)$ is 'corrected' by an amount of $-(k+1)^2[u_n - u_h(0)]$ to account for the jump (see also Fig. 2.1). In other words, by employing the $k+1$ left Radau points to evaluate the derivative of u_h, all the corrections caused by the jump $[u_n - u_h(0)]$ in function values at the left boundary is lumped to the left boundary itself and the amount of correction for the derivative evaluation at the left boundary is $-(k+1)^2[u_n - u_h(0)]$. This discussion will be clarified further by the correction function of the next subsection.

As a consequence of (2.16) and (2.17), the solution u_h can be constructed from the values of f_h at the left Radau points as follows. Consider k of the $k+1$ left Radau points away from the left boundary, namely, $\xi_{L,j}$, $2 \le j \le k+1$. Let $l_{L,2}^{(k-1)}$, …, $l_{L,k+1}^{(k-1)}$ be the corresponding Lagrange (basis) polynomials, which are of degree $k-1$. Then, by (2.16) and, since u_h' is of degree $k-1$,

$$u_h'(\xi) = \sum_{j=2}^{k+1} f_h(\xi_{L,j}) l_{L,j}^{(k-1)}(\xi). \tag{2.18}$$

Therefore,

$$u_h'(0) = \sum_{j=2}^{k+1} f_h(\xi_{L,j}) l_{L,j}^{(k-1)}(0).$$

Substitute right-hand side the above into (2.17), we obtain

$$u_h(0) = u_n + \frac{1}{(k+1)^2}\left[f_h(0) - \sum_{j=2}^{k+1} f_h(\xi_{L,j}) l_{L,j}^{(k-1)}(0)\right]. \tag{2.19}$$

Since $u_h(\xi) = u_h(0) + \int_0^\xi u_h'(\eta)\, d\eta$, the above and (2.18) yield a solution that depends only on $f_h(\xi_{L,j})$,

$$u_h(\xi) = u_h(0) + \int_0^\xi \sum_{j=2}^{k+1} f_h(\xi_{L,j}) l_{L,j}^{(k-1)}(\eta)\ d\eta. \tag{2.20}$$

Whereas u_h can be expressed using the values of f_h at the left Radau points as in the above two equations, it turns out that by using the right Radau points, u_h can be expressed in a simpler and more conveying manner as will be shown by (2.34) or (2.35) below.

Correction Function g

The polynomial γ approximates the derivative of a jump. We now wish to approximate the jump itself. In other words, we wish to integrate (2.14) by first integrating $-\gamma$.

Let the polynomial g of degree $k+1$ be defined by

$$g' = -\gamma = -(k+1)^2 l_{L,1} \tag{2.21}$$

and

$$g(0) = 1. \tag{2.22}$$

These two conditions result in

$$g(\xi) = 1 - \int_0^\xi (k+1)^2 l_{L,1}(\eta) d\eta. \tag{2.23}$$

The function g defined above satisfies

$$g(1) = 0. \tag{2.24}$$

Indeed, by using the left Radau quadrature and (2.12),

$$\int_0^1 (k+1)^2 l_{L,1}(\xi) d\xi = 1.$$

The above (which is also a property of the Dirac delta function) and (2.23) imply (2.24).

As a consequence of $g(0) = 1$ and $g' = -\gamma$, similar to (2.17), loosely put, when calculating the derivative of a jump at $\xi = 0$, a jump of size 1 in function values (i.e., $g(0) = 1$) leads to a jump of size $-(k+1)^2$ in derivative values (i.e., $g'(0) = -(k+1)^2$).

The following assertion holds: the polynomial g defined by (2.23) of degree $k+1$ is orthogonal to all polynomials of degree $k-1$ or less:

$$g \perp \boldsymbol{P}_{k-1}. \tag{2.25}$$

For the proof, let v be in $\boldsymbol{P}_k$, then v' is in $\boldsymbol{P}_{k-1}$ and, as v spans $\boldsymbol{P}_k$, v' spans $\boldsymbol{P}_{k-1}$. Next, recall that $g(0) = 1$ and $g(1) = 0$; thus

$$(g, v') = g(1)v(1) - g(0)v(0) - (g', v) = -v(0) - (g', v).$$

By (2.21), $g' = -\gamma$. Therefore,

$$(g', v) = (-\gamma, v) = -v(0),$$

where the last equality above follows from (2.10). As a result of the above two equations, for all v in $\boldsymbol{P}_k$,

$$(g, v') = 0.$$

As v spans $\boldsymbol{P}_k$, v' spans $\boldsymbol{P}_{k-1}$, and assertion (2.25) follows.

We can now show that g defined by (2.23) is identical to the right Radau polynomial of degree $k+1$ defined by the $k+2$ conditions that it vanishes at the $k+1$ right Radau points and $g(0) = 1$.

Indeed, condition $g(0) = 1$ is satisfied by requirement (2.22). Next, let the $k+1$ right Radau points be denoted by $\xi_{R,1}$, …, $\xi_{R,k+1}$. Among these points, $g\left(\xi_{R,k+1}\right) = g(1) = 0$ by (2.24). Consider now the k members other than the right boundary, namely, $\xi_{R,1}$, …, $\xi_{R,k}$. Let $l_{R,i}^{(k-1)}$, $1 \le i \le k$, be the corresponding Lagrange polynomials of degree $k-1$. Then, since, by (2.25), g is orthogonal to $\boldsymbol{P}_{k-1}$,

$$\left(g, l_{R,i}^{(k-1)}\right) = 0.$$

Next, evaluate $(g, l_{R,i}^{(k-1)})$ by the $k+1$ right Radau quadrature. Since $g(1) = 0$ and $l_{R,i}^{(k-1)}\left(\xi_{R,j}\right) = \delta_{ij}$ for $1 \le i, j \le k$, we obtain, with $b_{R,i}$ the Radau weight at $\xi_{R,i}$,

$$\left(g, l_{R,i}^{(k-1)}\right) = b_{R,i} g\left(\xi_{R,i}\right) l_{R,i}^{(k-1)}\left(\xi_{R,i}\right) = b_{R,i} g\left(\xi_{R,i}\right).$$

The above two equations imply $b_{R,i} g\left(\xi_{R,i}\right) = 0$. Since all Radau weights are nonzero (strictly positive),

$$g\left(\xi_{R,i}\right) = 0.$$

This completes the proof.

Fig. 2.3a shows the cubic correction function g for the case $k = 2$; here, g' vanishes at two of the three left Radau points: $g'\left(\xi_{L,2}\right) = g'\left(\xi_{L,3}\right) = 0$. Fig. 2.3b shows the correction function of degree $k+1$ for $k = 8$ (thin blue curve) and $k = 9$ (thick red curve).

The following remark is in order. In our context, the Heaviside function H on $[0, 1]$ is the step-up function defined by $H(0) = 0$ and $H(\xi) = 1$ for $0 < \xi \le 1$. Then $H' = \delta_0$ or H is the integral of δ_0. Let the step-down function be defined by $\mathrm{Stdn} = 1 - H$ or $\mathrm{Stdn}(0) = 1$ and, for $0 < \xi \le 1$, $\mathrm{Stdn}(\xi) = 0$. Then, $\mathrm{Stdn}' = -\delta_0$. Concerning the corresponding polynomial approximations, g of degree $k+1$ approximates the step-down function, and $g' = -\gamma$ of degree k approximates $-\delta_0$.

The correction function g can also be defined by using the Legendre polynomials, which are typically defined on $[-1, 1]$. Any function V on $[-1, 1]$ corresponds to a function $v(\xi)$ on $[0, 1]$ by

$$v(\xi) = V(2\xi - 1).$$

All special polynomials discussed here are on $[0, 1]$ using the above transformation. For any integer $n \ge 0$ (n here has nothing to do with the subscript n of u_n), the Legendre polynomial of degree n denoted by L_n is defined by the $n+1$ conditions that $L_n(1) = 1$ and L_n is orthogonal to $\boldsymbol{P}_{n-1}$. Then, as is well known,

$$L_n(0) = (-1)^n.$$

Next, the left and right Radau polynomials of degree n are respectively defined by

$$R_{L,n} = \frac{1}{2}(L_n + L_{n-1}) \text{ and } R_{R,n} = \frac{(-1)^n}{2}(L_n - L_{n-1}). \tag{2.26}$$

Note that $R_{R,n}(\xi) = R_{L,n}(1-\xi)$. The above definitions imply

$$R_{L,n}(0) = 0,\ R_{L,n}(1) = 1,\ R_{R,n}(0) = 1, \text{ and } R_{R,n}(1) = 0.$$

The correction function g equals the right Radau polynomial of degree $k+1$ (see Huynh 2007, 2009a):

$$g = R_{R,k+1}. \tag{2.27}$$

Also note that since $L_n \perp \boldsymbol{P}_{n-1}$ for all n, by the second half of (2.26), g above satisfies $g \perp \boldsymbol{P}_{k-1}$, consistent with (2.25).

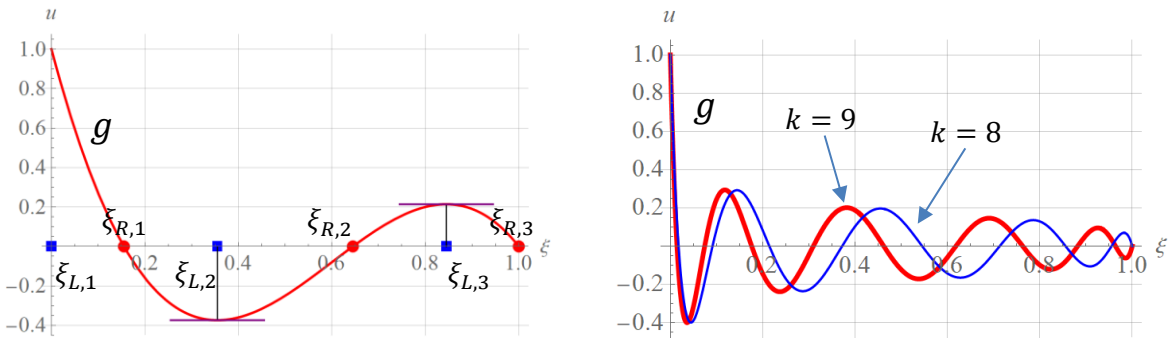

(a) **(b)**

Fig. 2.3 (a) The cubic correction function g for the case $k = 2$; g vanishes at the three right Radau points (red round dots) and has local extrema at two of the three left Radau points (blue square dots). **(b)** The correction functions of degree $k+1$ for $k = 9$ (thick red curve) and $k = 8$ (thin blue curve).

Fig. 2.4 shows, on $[0, 1]$, the graphs of the Legendre polynomials of degree n (thin blue curve) and degree $n-1$ (thin purple curve), the left Radau polynomial of degree n or $R_{L,n} = (L_n + L_{n-1})/2$ (dashed red curve) , and the right Radau polynomial $R_{R,n}$ (thick red curve); Fig. 2.4a depicts the case $n = 2$ and Fig. 2.4b the case $n = 3$. The zeros of the right Radau polynomial are the right Radau points (red round dots), and the zeros of the left Radau polynomial are the left Radau points (blue square dots). The interior left Radau points (the exception is the first one, $\xi = 0$) are the local extrema of the right Radau polynomial and, vice versa, the interior right Radau points (the exception is the last one, $\xi = 1$) are the local extrema of the left Radau polynomial. The abscissas of the intersections of the curves L_{n-1} and L_n are also the interior right Radau points.

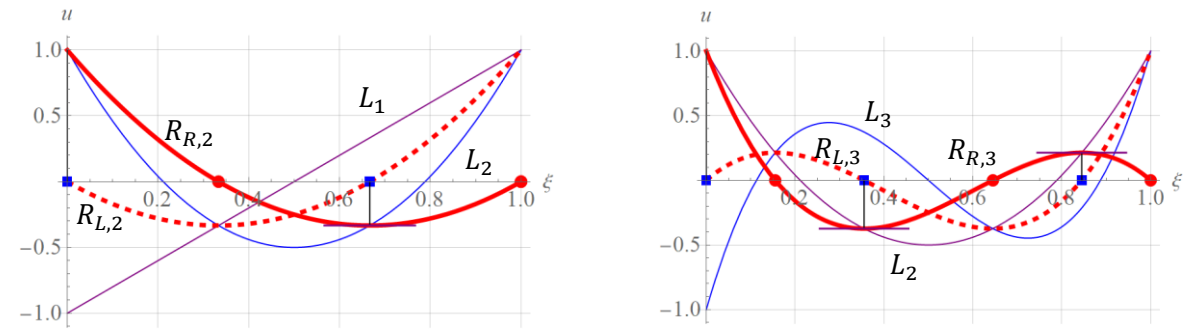

(a) **(b)**

Fig. 2.4 The graphs of L_n (thin blue curve), L_{n-1} (thin purple curve), $R_{L,n}$ (dashed red curve), and $R_{R,n}$ (thick red curve) for **(a)** $n = 2$ and **(b)** $n = 3$.

Note that the Radau polynomials were employed in the flux reconstruction method to correct for the jumps in fluxes at the cell boundaries (Huynh 2007, 2009a, Huynh, Wang, & Vincent 2014). They were employed for error estimates in Baccouch (2016) to prove the super-convergence properties.

We review the key properties of g. It is of degree $k+1$ so that g' is of degree k matching that of u_h and f_h. It vanishes at the $k+1$ right Radau points; on the other hand, g' vanishes at k of the $k+1$ left Radau points; the exception is $g'(0) = -(k+1)^2$. It provides a polynomial approximation to the step-down function. The polynomial $-g' = \gamma = (k+1)^2 l_{L,1}$ of degree k approximates δ_0. Finally, g is the polynomial of degree $k+1$ defined by the $k+2$ conditions that $g(0) = 1$, $g(1) = 0$, and $g \perp \boldsymbol{P}_{k-1}$.

DG Formulation via Correction Function

We can now apply the correction function g to the DG formulation.

To prepare for the resulting implicit Runge-Kutta methods, from here on, we deal with the equation $u' = du/d\xi = hf$ and a general step size h. By (2.21), $g' = -\gamma$; therefore, (2.14) takes the form

$$([u_n - u_h(0)]g + u_h)' = hf_h. \tag{2.28}$$

Next, set

$$U = [u_n - u_h(0)]g + u_h. \tag{2.29}$$

Then U is of degree $k+1$ whereas u_h is of degree k, and (2.28) can be written concisely:

$$U' = hf_h. \tag{2.30}$$

Eq. (2.29) implies, since $g(0) = 1$,

$$U(0) = u_n \tag{2.31}$$

and, since $g(1) = 0$,

$$U(1) = u_h(1). \tag{2.32}$$

The polynomial U defined by (2.29) solves the ODE by matching it closely as shown by (2.30) and (2.31). At the $k+1$ right Radau points, the values of U match those of u_h, i.e., for $1 \le i \le k+1$,

$$U(\xi_{R,i}) = u_h(\xi_{R,i}). \tag{2.33}$$

Thus, u_h can be defined by $U(\xi_{R,i})$, $1 \le i \le k+1$, and vice versa, U can be defined by the starting condition u_n and the values $u_h(\xi_{R,i})$ at the right Radau points; U can also be defined by the $k+2$ conditions of $U(0) = u_n$ and $U(1) = u_h(1)$ at the two ends, and the k conditions that U is as close as possible to u_h in the sense that they have the same projection onto $\boldsymbol{P}_{k-1}$ (a consequence of (2.29) and $g \perp \boldsymbol{P}_{k-1}$).

As a result of (2.30) and (2.31), with ξ varies on $[0, 1]$,

$$U(\xi) = u_n + h\int_0^\xi f_h(\eta, u_h(\eta))d\eta. \tag{2.34}$$

Thus, if $f_h = \mathcal{P}_k(f)$ is known via a quadrature rule or exact integration, U can be obtained by the above.

The solution u_h satisfies, by the above and (2.29),

$$[u_n - u_h(0)]g(\xi) + u_h(\xi) = u_n + h\int_0^\xi f_h(\eta, u_h(\eta))d\eta. \tag{2.35}$$

Since f_h depends on u_h, the above results in an implicit system of equations discussed in the next section. At x_{n+1}, or $\xi = 1$, the solution is

$$u_{n+1} = u_h(1) = U(1) = u_n + h\int_0^1 f_h(\eta, u_h(\eta))d\eta. \tag{2.36}$$

The relation among the solution U and the collocation, as well as CG solutions, is discuss below.

To prepare, with ξ on $[0, 1]$, consider the ODE $u'(\xi) = du/d\xi = hf(\xi, u(\xi))$ and $u(0) = u_n$.

In the case of collocation, let η_i, $1 \le i \le k+1$, be strictly increasing values on $[0, 1]$. The collocation method with collocation points η_i seeks a polynomial solution $\mathcal{U}$ of degree $k+1$ satisfying

$$\mathcal{U}(0) = u_n, \tag{2.37}$$

and, for $1 \le i \le k+1$,

$$\mathcal{U}'(\eta_i) = hf(\eta_i, \mathcal{U}(\eta_i)). \tag{2.38}$$

The CG method seeks a polynomial of degree $k+1$, also denoted by $\mathcal{U}$, that satisfies (2.37) and, for any v in $\boldsymbol{P}_k$,

$$(\mathcal{U}', v) = h(f(\xi, \mathcal{U}(\xi)), v). \tag{2.39}$$

The solution at x_{n+1} for either method is $\mathcal{U}(1)$.

Let l_i, $1 \le i \le k+1$, be the Lagrange polynomials corresponding to η_i's. Then under the quadrature associated with η_i's, the above with $v = l_i$ implies (2.38), which results in the following claim.

The CG method using the quadrature associated with the collocation points and the corresponding collocation method yield identical solutions.

For later use, under the quadrature associated with the collocation points, the CG and collocation solution satisfies, by the above claim and by (2.39),

$$\mathcal{U}' = h\mathcal{P}_k\big(f(\xi, \mathcal{U}(\xi))\big). \tag{2.40}$$

Proposition 2.1. Under the right Radau quadrature, the DG solution U defined by (2.29) is identical to the right Radau collocation solution as well as the CG solution under the same quadrature.

Indeed, at each right Radau point $\xi_{R,i}$, $1 \le i \le k+1$, since $g\big(\xi_{R,i}\big) = 0$, by (2.29),

$$U\big(\xi_{R,i}\big) = u_h(\xi_{R,i}). \tag{2.41}$$

Therefore, $f\big(\xi_{R,i}, u_h(\xi_{R,i})\big) = f\big(\xi_{R,i}, U(\xi_{R,i})\big)$. Next, under the right Radau quadrature, $f_h = \mathcal{P}_k(f)$ is determined by the $k+1$ values $f\big(\xi_{R,i}, u_h(\xi_{R,i})\big)$ (see also (3.5) below). As a result, for $1 \le i \le k+1$,

$$f_h\big(\xi_{R,i}, u_h(\xi_{R,i})\big) = f\big(\xi_{R,i}, u_h(\xi_{R,i})\big) = f\big(\xi_{R,i}, U(\xi_{R,i})\big). \tag{2.42}$$

Consequently, for $1 \le i \le k+1$, (2.30) implies,

$$U'\big(\xi_{R,i}\big) = hf\big(\xi_{R,i}, U(\xi_{R,i})\big). \tag{2.43}$$

Thus, the DG solution U of degree $k+1$ can be defined by the $k+2$ conditions of $U(0) = u_n$ and the above, which is exactly the definition (2.38) of the collocation solution with $\mathcal{U}$ replaced by U. The claim after (2.39) shows that the collocation solution is the same as the CG solution under the quadrature with collocation points as quadrature points. See also Huynh (2009b). This completes the proof.

The above discussion shows that the right Radau quadrature is a convenient and sensible choice of quadrature for the DG method in the context of ODEs. (It is important to note that this comment does not hold in the context of conservation laws, where upwinding at each interface can involve values from both sides, not just by the value from the left as is the case here). Below, however, the quadrature can be the left or right Radau, Gauss, or a blending of the Radau quadratures where the evaluation points are the zeros of Q defined by, with $0 \le \alpha \le 1$,

$$Q = \alpha R_{R,k+1} + (1-\alpha)(-1)^{k+1} R_{L,k+1}. \tag{2.44}$$

Such a quadrature, with $k+1$ evaluation points, has a degree of precision $2k$ or higher.

Concerning the two DG solutions u_h and U, if an approximation at ξ for $0 < \xi < 1$ is needed, $U(\xi)$ is generally a better choice than $u_h(\xi)$. The values of u_h at the right Radau points are more accurate than those at other points since they match the values of U (of one degree higher). What is crucial, however, is that at $\xi = 1$, U and u_h yield the same solution u_{n+1}, which is accurate to order $2k+1$, the order of accuracy of the right Radau quadrature. On the other hand, the expected order of accuracy for a quadrature using a polynomial approximation of degree k is only $k+1$. The property of much higher accuracy order than expected is also called 'super convergence' (e.g., Adjerid et al. 2002, Baccouch 2016).

As a passing remark, the correction function g was employed to reconstruct the flux for conservation laws in the flux reconstruction or FR method (Huynh 2007, 2009a, Huynh, Wang, and Vincent 2014). The method, in turn, is used in codes applied to practical calculations such as PyFR (https://www.pyfr.org/) and GFR (Spiegel et al. 2022). Here, the function u itself is being reconstructed from u_h in the form of U. Thus, the above formulation can be considered as the FR, or 'function reconstruction', approach for ODE.

3 Implicit Runge-Kutta Methods Resulting from DG Formulation

We next construct the implicit Runge-Kutta method resulting from the DG formulation or IRK-DG. Here, the correction function g plays a crucial role. To be consistent with the standard RK notation, let the number of stages be

$$s = k + 1.$$

A quadrature on $[0, 1]$ with s evaluation points $\xi_1, \ldots, \xi_s$ and a degree of precision $2s - 2$ or higher is employed, e.g., the left or right Radau, Gauss, or a blending of the Radau quadratures via (2.44). Denote the corresponding Lagrange polynomials by l_j, $1 \le j \le s$, which are of degree $s - 1$ and defined by $l_j(\xi_i) = \delta_{ij}$. Then, for each j, the quadrature weight is

$$b_j = \int_0^1 l_j(\xi) d\xi. \tag{3.1}$$

Note that even if the Legendre polynomials are employed as basis functions for the DG formulation, we still need a quadrature to evaluate inner products. Since the quadrature is assumed to be exact for polynomials of degree $2s - 2$ or less, and $l_i l_j$ is of degree $2s - 2$, for $1 \le i, j \le s$,

$$\left(l_i, l_j\right) = \delta_{ij} b_j, \tag{3.2}$$

Thus, l_j, $j = 1, \ldots, s$, form an orthogonal basis for $\boldsymbol{P}_{s-1}$.

At each quadrature point ξ_j, set

$$u_{n,j} = u_h(\xi_j) \quad \text{and} \quad f_{n,j} = f(\xi_j, u_{n,j}). \tag{3.3}$$

Then, the solution u_h of degree $s - 1$ can be expressed as

$$u_h(\xi) = \sum\nolimits_{j=1}^{s} u_{n,j}\, l_j(\xi). \tag{3.4}$$

Concerning a similar expression for $f_h = \mathcal{P}_{s-1}(f)$, whereas u_h is a polynomial, $f\left(\xi, u_h(\xi)\right)$ can be a non-polynomial. Since l_j, $j = 1, \ldots, s$, form an orthogonal basis for $\boldsymbol{P}_{s-1}$,

$$\mathcal{P}_{s-1}(f) = \sum\nolimits_{j=1}^{s} \frac{\left(f, l_j\right)}{\left(l_j, l_j\right)} l_j.$$

By using the quadrature, $\left(f, l_j\right) = \int_0^1 f\left(\xi, u_h(\xi)\right) l_j(\xi) d\xi = b_j f_{n,j}$. As a result of (3.2) and the above, under the quadrature with evaluation points ξ_j's,

$$\mathcal{P}_{s-1}(f)(\eta) = (\mathcal{P}_{s-1}(f))(\eta) = f_h(\eta) = \sum\nolimits_{j=1}^{s} f_{n,j}\, l_j(\eta). \tag{3.5}$$

Next, set

$$\tilde{l}_j(\xi) = \int_0^{\xi} l_j(\eta) d\eta \tag{3.6}$$

and

$$\tilde{f}_h(\xi) = \int_0^{\xi} f_h(\eta) d\eta. \tag{3.7}$$

Then, for each fixed ξ, the quantities $\tilde{l}_j(\xi)$, $1 \le j \le s$, are the weights at ξ_j for a quadrature from 0 to ξ:

$$\int_0^{\xi} f_h(\eta) d\eta = \tilde{f}_h(\xi) = \sum\nolimits_{j=1}^{s} f_{n,j}\, \tilde{l}_j(\xi). \tag{3.8}$$

If $\xi = 1$, the quadrature weights are, by (3.1),

$$\tilde{l}_j(1) = b_j, \tag{3.9}$$

and the degree of precision for the corresponding quadrature is $2s-2$ or higher as in our assumption. For $\xi \neq 1$, however, the quadrature (3.8) has a degree of precision of only $s-1$.

Fig. 3.1a shows, for the case $s=3$, the cubics $\tilde{l}_j$, $1 \le j \le 3$; here, the quadrature points are the 3 left Radau points; the quadratic l_j used in (3.6) to construct $\tilde{l}_j$ for this case is identical to $l_{L,j}$ of Fig. 2.2a.

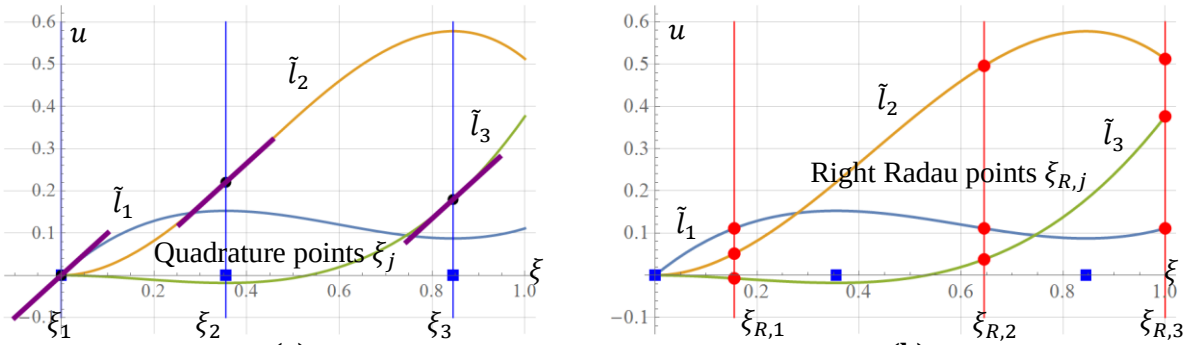

Fig. 3.1 (a) The polynomials $\tilde{l}_j$ for the case the quadrature points are the 3 left Radau points (blue square dots); **(b)** the values $\tilde{l}_j(\xi_{R,i})$, $1 \le i,j \le 3$, i.e., the entries of the matrix $\boldsymbol{M}_{RI}$, are represented by the red round dots; the values at the red round dots on the vertical line at each right Radau points $\xi = \xi_{R,i}$ form the entries for the i-th row of $\boldsymbol{M}_{RI}$.

Assume for the moment, the values $u_{n,j}$ at the quadrature points ξ_j are known, $1 \le j \le s$; therefore, $f_{n,j} = f(\xi_j, u_{n,j})$ are also known. Using (3.4) and (3.5), Eq. (2.35) implies

$$\left[u_n - \sum_{j=1}^{s} u_{n,j}\, l_j(0)\right] g(\xi) + \sum_{j=1}^{s} u_{n,j}\, l_j(\xi) = u_n + h \sum_{j=1}^{s} f_{n,j} \int_0^{\xi} l_j(\eta)\, d\eta. \qquad (3.10)$$

Note that the above equation involves no inner product since $f_h = \mathcal{P}_{s-1}(f)$ is defined by $f_{n,j}$.

Our goal is to obtain an implicit system of equations for $u_{n,i}$, $1 \le i \le s$, as shown below in (3.22) (these values define u_h). To this end, at each right Radau point $\xi_{R,i}$, since $g(\xi_{R,i}) = 0$, by evaluating the above at $\xi_{R,i}$ and by using (3.6),

$$\sum_{j=1}^{s} u_{n,j}\, l_j(\xi_{R,i}) = u_n + h \sum_{j=1}^{s} f_{n,j}\, \tilde{l}_j(\xi_{R,i}). \qquad (3.11)$$

Note (3.11) does *not* hold at points other than right Radau.

Concerning the left-hand side above, with 'R' for 'right' Radau or 'row', and 'Q' for 'quadrature' or 'column', denote the matrix

$$\boldsymbol{M}_{RQ} = \{l_j(\xi_{R,i})\}_{i,j=1}^{s}. \qquad (3.12)$$

For the following row vectors of values at quadrature points, denote the corresponding column vectors by

$$\boldsymbol{u}_n = \left((u_{n,j})_{j=1}^{s}\right)^T, \quad \boldsymbol{f}_n = \left((f_{n,j})_{j=1}^{s}\right)^T, \text{ and } \mathbf{1} = (1,1,\ldots 1)^T$$

where the superscript 'T' represents the transpose. When it does not cause confusion, we simply use the index i and the notation $(u_{n,i})_{i=1}^{s}$ for a column vector. Then, by (3.4), the left-hand side of (3.11) implies

$$\left(u_h(\xi_{R,i})\right)_{i=1}^{s} = \left(\sum_{j=1}^{s} u_{n,j}\, l_j(\xi_{R,i})\right)_{i=1}^{s} = \boldsymbol{M}_{RQ} \cdot \boldsymbol{u}_n. \qquad (3.13)$$

That is, with $\boldsymbol{u}_n$ the (column) vector of values at the quadrature points, which determines u_h, the vector of values of u_h at the right Radau points is given by the matrix-vector product $\boldsymbol{M}_{RQ} \cdot \boldsymbol{u}_n$.

Concerning the right-hand side of (3.11), with 'R' for 'right' Radau and 'I' for 'integral', denote

$$\boldsymbol{M}_{RI} = \left\{ \int_0^{\xi_{R,i}} l_j(\eta) d\eta \right\}_{i,j=1}^{s} = \left\{ \tilde{l}_j(\xi_{R,i}) \right\}_{i,j=1}^{s}. \tag{3.14}$$

As in (3.8), for each fixed i, the i-th row of $\boldsymbol{M}_{RI}$, i.e., the row vector $\left\{ \tilde{l}_j(\xi_{R,i}) \right\}_{j=1}^{s}$, provides the weights for a quadrature formula with evaluation points ξ_j, $1 \le j \le s$, for the integral from 0 to $\xi_{R,i}$:

$$\int_0^{\xi_{R,i}} f_h(\eta) d\eta = \tilde{f}_h(\xi_{R,i}) = \sum\nolimits_{j=1}^{s} f_{n,j}\, \tilde{l}_j(\xi_{R,i}).$$

The quadrature formula has a degree of precision of only $s-1$, except when $i = s$, where the degree of precision is $2s-2$ or $2s-1$. The rightmost hand side above is the i-th row of the vector $\boldsymbol{M}_{RI} \cdot \boldsymbol{f}_n$, and

$$\left(\tilde{f}_h(\xi_{R,i}) \right)_{i=1}^{s} = \boldsymbol{M}_{RI} \cdot \boldsymbol{f}_n. \tag{3.15}$$

That is, multiplying by $\boldsymbol{M}_{RI}$ (on the left) yields the vector of the integration from 0 to the right Radau points. For later use, concerning the components, with each fixed j, by replacing f_h by l_j in the above,

$$\left(\tilde{l}_j(\xi_{R,i}) \right)_{i=1}^{s} = \boldsymbol{M}_{RI} \cdot \left(l_j(\xi_i) \right)_{i=1}^{s}. \tag{3.16}$$

Here, the column vector $\left(l_j(\xi_i) \right)_{i=1}^{s}$ has all zero entries except the j-th entry, i.e., i-th row where $i = j$, which equals 1 since $l_j(\xi_i) = \delta_{ij}$, and the right-hand side above yields the j-th column of $\boldsymbol{M}_{RI}$.

Fig. 3.1b shows the entries of $\boldsymbol{M}_{RI}$ as red round dots (corresponding to the setting in Fig. 3.1a). Here, again the quadrature points are the 3 left Radau points. For each fixed i, the i-th row of $\boldsymbol{M}_{RI}$ consists of the values of the three red round dots on the vertical line through the right Radau point $\xi = \xi_{R,i}$. For each fixed j, the j-th column of $\boldsymbol{M}_{RI}$ consists of the values of the three red round dots on the curve $\tilde{l}_j$.

Continuing with the derivation of the IRK method, using (3.13) and (3.15), Eq. (3.11) implies

$$\boldsymbol{M}_{RQ} \cdot \boldsymbol{u}_n = u_n \boldsymbol{1} + h\, \boldsymbol{M}_{RI} \cdot \boldsymbol{f}_n. \tag{3.17}$$

To obtain $\boldsymbol{M}_{RQ}^{-1}$, denote the Lagrange polynomials for the right Radau points by $l_{R,j}$, $1 \le j \le s$. Set

$$\boldsymbol{M}_{QR} = \left\{ l_{R,j}(\xi_i) \right\}_{i,j=1}^{s}. \tag{3.18}$$

Suppose the vector $\boldsymbol{v}$ of the s values $v_{R,1}$, …, $v_{R,s}$ at the right Radau points is known; $\boldsymbol{v}$ determines a polynomial v of degree $s-1$. The vector of values of v at the quadrature points is given by $\boldsymbol{M}_{QR} \cdot \boldsymbol{v}$.

With $\boldsymbol{I}$ denoting the $s \times s$ identity matrix, we next show that

$$\boldsymbol{M}_{QR} \cdot \boldsymbol{M}_{RQ} = \boldsymbol{I}. \tag{3.19}$$

Indeed, let w be a polynomial of degree $s-1$, and let $\boldsymbol{w}_Q$ be the vector of values of w at the quadrature points. Then $\boldsymbol{w}_R = \boldsymbol{M}_{RQ} \cdot \boldsymbol{w}_Q$ is the vector of values of w at the right Radau points, and $\boldsymbol{w}_R$ also defines a polynomial identical to w. Next, the vector of values of w at the quadrature points is given by $\boldsymbol{M}_{QR} \cdot \boldsymbol{w}_R$, which is identical to $\boldsymbol{w}_Q$; thus, (3.19) follows.

The constant function 1 takes on the value 1 at all points, as a result,

$$\boldsymbol{M}_{QR} \cdot \boldsymbol{1} = \boldsymbol{M}_{RQ} \cdot \boldsymbol{1} = \boldsymbol{1}.$$

Multiply (3.17) on the left by $\boldsymbol{M}_{QR}$ and using the above two equations, we obtain

$$\boldsymbol{u}_n = u_n \boldsymbol{1} + h\, \boldsymbol{M}_{QR} \cdot \boldsymbol{M}_{RI} \cdot \boldsymbol{f}_n, \tag{3.20}$$

where $\boldsymbol{u}_n = \left(u_{n,i} \right)_{i=1}^{s}$ and $\boldsymbol{f}_n = \left(f_{n,i} \right)_{i=1}^{s}$. Next, set

$$\boldsymbol{A} = \boldsymbol{M}_{QR} \cdot \boldsymbol{M}_{RI}, \tag{3.21}$$

Then the resulting IRK-DG method follows from (3.20):

$$\boldsymbol{u}_n = u_n \boldsymbol{1} + h\, \boldsymbol{A} \cdot \boldsymbol{f}_n. \tag{3.22}$$

In summary, the DG method using a quadrature with s evaluation points ξ_i's and of a degree of precision $2s-2$ or higher results in an s-stage IRK scheme with a Butcher tableau (see also Table 3.1 below) defined by, for $1 \le i,j \le s$, the stages $c_i = \xi_i$ (leftmost column), the quadrature weights b_j at ξ_j (bottom row), and with $\boldsymbol{M}_{QR}$ by (3.18) and $\boldsymbol{M}_{RI}$ by (3.14), the matrix $\boldsymbol{A}$ (upper right matrix) where

$$\boldsymbol{A} = \left(a_{ij}\right)_{i,j=1}^{s} = \boldsymbol{M}_{QR} \cdot \boldsymbol{M}_{RI}. \tag{3.23}$$

Eq. (3.22) can be written in a more familiar form: for $1 \le i \le s$,

$$u_{n,i} = u_n + h \sum_{j=1}^{s} a_{i,j} f\left(\xi_j, u_{n,j}\right). \tag{3.24}$$

With $u_{n,i}$ by the above implicit system of equations, and $f_{n,j} = f(\xi_j, u_{n,j})$, the solution is given by

$$u_{n+1} = u_n + h \sum_{j=1}^{s} b_j f_{n,j}. \tag{3.25}$$

The vector $\boldsymbol{M}_{QR} \cdot \boldsymbol{M}_{RI} \cdot \boldsymbol{f}_n = \boldsymbol{A} \cdot \boldsymbol{f}_n$ in (3.20) plays an important role. Its meaning is discussed below.

The vector $\boldsymbol{M}_{RI} \cdot \boldsymbol{f}_n = \left(\tilde{f}_h(\xi_{R,i})\right)_{i=1}^{s}$ given by (3.15) is the vector of values of $\tilde{f}_h$ at the s right Radau points. These s values define a polynomial of degree $s-1$ denoted by r, which is generally different from $\tilde{f}_h$ of degree s. Then, $\boldsymbol{M}_{QR} \cdot \left(\tilde{f}_h(\xi_{R,i})\right)_{i=1}^{s}$ yields the vector of values of r at the quadrature points:

$$\left(r(\xi_i)\right)_{i=1}^{s} = \boldsymbol{M}_{QR} \cdot \boldsymbol{M}_{RI} \cdot \boldsymbol{f}_n = \boldsymbol{A} \cdot \boldsymbol{f}_n. \tag{3.26}$$

Concerning the components, for each fixed j, the s values $\tilde{l}_j(\xi_{R,i})$ at the right Radau points, $1 \le i \le s$, define a polynomial denoted by r_j of degree $s-1$, which is different from $\tilde{l}_j$ of degree s; and

$$\left(r_j(\xi_i)\right)_{i=1}^{s} = \boldsymbol{M}_{QR} \cdot \left(\tilde{l}_j(\xi_{R,i})\right)_{i=1}^{s} = \boldsymbol{M}_{QR} \cdot \boldsymbol{M}_{RI} \cdot \left(l_j(\xi_i)\right)_{i=1}^{s} \tag{3.27}$$

where the second equality follows from (3.16). Since $\boldsymbol{M}_{QR} \cdot \boldsymbol{M}_{RI} = \boldsymbol{A}$, the above implies

$$\left(r_j(\xi_i)\right)_{i=1}^{s} = \boldsymbol{A} \cdot \left(l_j(\xi_i)\right)_{i=1}^{s}.$$

Since $l_j(\xi_i) = \delta_{ij}$, for each fixed j, the product $\boldsymbol{A} \cdot \left(l_j(\xi_i)\right)_{i=1}^{s}$ yields the j-th column of $\boldsymbol{A}$. In other words, for $1 \le i,j \le s$,

$$a_{ij} = r_j(\xi_i). \tag{3.28}$$

The above argument implies that multiplying a vector $\boldsymbol{f}_n$ by $\boldsymbol{A}$ (on the left) yields a vector, which is an approximation (via r) to the integration of f_h from 0 to the quadrature points ξ_i, $1 \le i \le s$. In other words, $\boldsymbol{A}$ corresponds to quadrature formulas: for each fixed i, the i-th row of $\boldsymbol{A}$ corresponds to the weights of a quadrature formula for the integration from 0 to ξ_i with quadrature points ξ_j and quadrature weights a_{ij}, $1 \le j \le s$. Due to the approximation by r_i, we expect a reduction in the degree of precision by 1 as will be discussed when dealing with condition $C(\eta)$ for accuracy after (4.3).

Regarding the solution u_h, using the above, Eq. (3.24) implies, for each i, $1 \le i \le s$,

$$u_{n,i} = u_n + h \sum_{j=1}^{s} f_{n,j} r_j(\xi_i).$$

Then, u_h of degree $s-1$, defined by the values $u_{n,i}$'s above at the quadrature points, is given by

$$u_h = u_n + h \sum_{j=1}^{s} f_{n,j}\, r_j.$$

That is, if $f_{n,j}$, $1 \le j \le s$, are known, the solution polynomial u_h can be obtained by the above.

Fig. 3.2 shows, for $s = 2$ (i.e., $k = 1$), the entries of $\boldsymbol{A}$ (big square dots) of the Butcher tableau. The IRK-DG method has quadrature points ξ_i's (small black squares) of type (a) left Radau, (b) Gauss, and (c) right Radau. For each fixed j, the quadratic $\tilde{l}_j$ is shown by the thin curve, and the values of $\tilde{l}_j$ at the two right Radau points are given by the two red round dots; these values determine a linear function r_j shown by the thick line. The two values $r_j(\xi_i)$ at the quadrature points ξ_i, $1 \le i \le 2$, shown as big square dots,

form the j-th column of the matrix $\boldsymbol{A}$. For each fixed i, the entries for the i-th row of $\boldsymbol{A}$ are represented by the large square dots on the vertical line $\xi = \xi_i$. Note that in Fig. 3.2c, since the quadrature points are also the right Radau points, the red round dots are identical to and appear on top of the large square dots.

Table 3.1 shows, for $s = 2$, the Butcher tableaux of the IRK-DG methods where, similar to Fig. 3.2, the quadrature is of type (a) left Radau, (b) Gauss, and (c) right Radau. Here, the values for the entries of $\boldsymbol{A}$ match the values at the large square dots of Fig. 3.2. Also note that Table 3.1a corresponds to the Radau IA method and Table 3.1c to Radau IIA (Ehle 1969, Axelsson 1969). The IRK-DG method of Table 3.1b, derived here constructively via the correction function, was derived algebraically in (Bottasso 1997, Tang & Sun 2012); it is called DG-Gauss here.

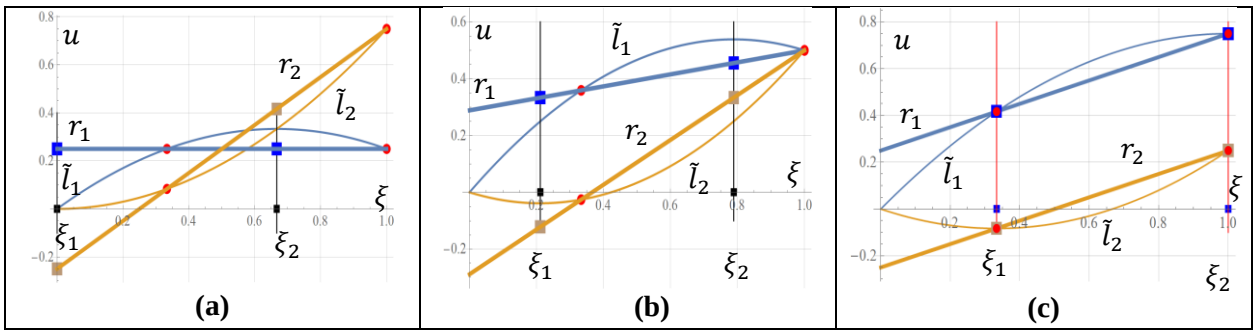

Fig. 3.2 The entries of $\boldsymbol{A}$ of the Butcher tableau for the DG method with $s = 2$ represented by big square dots; each i-th row of $\boldsymbol{A}$ corresponds to the values on the vertical line at $\xi = \xi_i$. The quadrature points ξ_i's (small black squares) are of type **(a)** left Radau, **(b)** Gauss, and **(c)** right Radau. The quadratic $\tilde{l}_j$ is shown by the thin curve, and the values of $\tilde{l}_j$ at the two right Radau points are given by the two red round dots; these values determine a linear function r_j shown by the thick line; and $\boldsymbol{A} = \{r_j(\xi_i)\}_{i,j=1}^{2}$.

Table 3.1 Butcher tableaux for the IRK-DG method with $s = 2$.

(a) Radau IA (left Radau)

0	$\frac{1}{4}$	$-\frac{1}{4}$
$\frac{2}{3}$	$\frac{1}{4}$	$\frac{5}{12}$
	$\frac{1}{4}$	$\frac{3}{4}$

(b) DG-Gauss

$\frac{1}{2}-\frac{\sqrt{3}}{6}$	$\frac{1}{3}$	$\frac{1-\sqrt{3}}{6}$
$\frac{1}{2}+\frac{\sqrt{3}}{6}$	$\frac{1+\sqrt{3}}{6}$	$\frac{1}{3}$
	$\frac{1}{2}$	$\frac{1}{2}$

(c) Radau IIA (right Radau)

$\frac{1}{3}$	$\frac{5}{12}$	$-\frac{1}{12}$
1	$\frac{3}{4}$	$\frac{1}{4}$
	$\frac{3}{4}$	$\frac{1}{4}$

The DG-Gauss method corresponding to Fig. 3.2b and Table 3.1b is, as will be discussed, third-order accurate. For comparison, the Gauss collocation method, which is fourth order accurate, has the same c_i's and b_j's, but $\{a_{11}, a_{12}\} = \left\{\frac{1}{4},\ \frac{1}{4}-\frac{\sqrt{3}}{6}\right\}$, and $\{a_{21}, a_{22}\} = \left\{\frac{1}{4}+\frac{\sqrt{3}}{6},\ \frac{1}{4}\right\}$; this method gains in accuracy and is also A-stable, but as opposed to IRK-DG, it has the disadvantage of *not* being L-stable (discussed later).

Fig. 3.3 is the analogous to Fig. 3.2 except $s = 3$. Again, for each fixed i, the entries for the i-th row of $\boldsymbol{A}$ are represented by the large square dots on the vertical line $\xi = \xi_i$.

Table 3.2 shows the Butcher tableaux of the IRK-DG methods with $s = 3$ where the quadrature is of type (a) left Radau and (b) right Radau. Again, the entries of $\boldsymbol{A}$ match the values at the large square dots of Figs. 3.3a and 3.3c. Tables 3.2a yields Radau IA and Table 3.2b yields Radau IIA methods.

Table 3.3 shows, again for $s = 3$, the Butcher tableaux for (a) the IRK-DG method with Gauss quadrature (accuracy order 5) and, for comparison, (b) the Gauss collocation method (accuracy order 6).

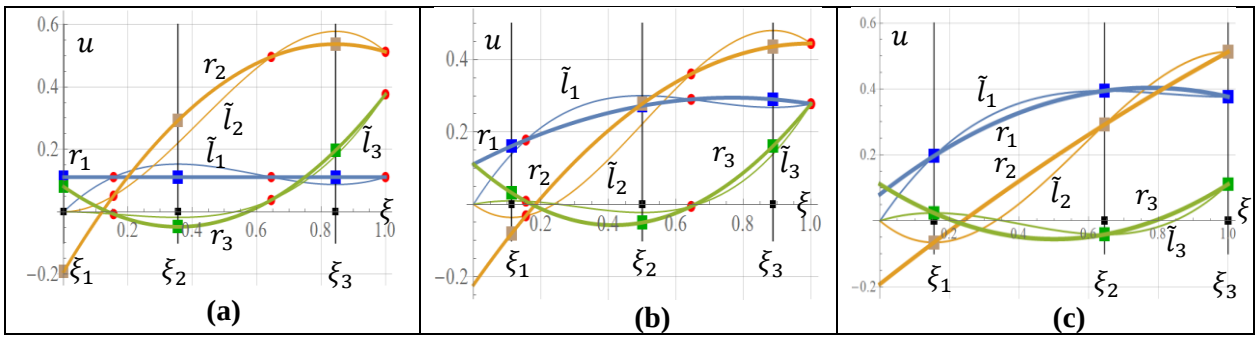

Fig. 3.3 The entries of $\boldsymbol{A}$ for the DG method with $s = 3$ represented by big square dots. The quadrature points ξ_i's (small black squares) are of type **(a)** left Radau, **(b)** Gauss, and **(c)** right Radau.

Table 3.2 Butcher tableaux for the IRK-DG methods with $s = 3$.

(a) Radau IA (left Radau)

0	$\frac{1}{9}$	$\frac{-1-\sqrt{6}}{18}$	$\frac{-1+\sqrt{6}}{18}$
$\frac{6-\sqrt{6}}{10}$	$\frac{1}{9}$	$\frac{88+7\sqrt{6}}{360}$	$\frac{88-43\sqrt{6}}{360}$
$\frac{6+\sqrt{6}}{10}$	$\frac{1}{9}$	$\frac{88+43\sqrt{6}}{360}$	$\frac{88-7\sqrt{6}}{360}$
	$\frac{1}{9}$	$\frac{16+\sqrt{6}}{36}$	$\frac{16-\sqrt{6}}{36}$

(b) Radau IIA (right Radau)

$\frac{4-\sqrt{6}}{10}$	$\frac{88-7\sqrt{6}}{360}$	$\frac{296-169\sqrt{6}}{1800}$	$\frac{-2+3\sqrt{6}}{225}$
$\frac{4+\sqrt{6}}{10}$	$\frac{296+169\sqrt{6}}{1800}$	$\frac{88+7\sqrt{6}}{360}$	$\frac{-2-3\sqrt{6}}{225}$
1	$\frac{16-\sqrt{6}}{36}$	$\frac{16+\sqrt{6}}{36}$	$\frac{1}{9}$
	$\frac{16-\sqrt{6}}{36}$	$\frac{16+\sqrt{6}}{36}$	$\frac{1}{9}$

Table 3.3 Butcher tableaux with $s = 3$

(a) DG-Gauss (order 5)

$\frac{1}{2}-\frac{\sqrt{15}}{10}$	$\frac{29}{180}$	$\frac{8-3\sqrt{15}}{45}$	$\frac{29-6\sqrt{15}}{180}$
$\frac{1}{2}$	$\frac{8+3\sqrt{15}}{72}$	$\frac{5}{18}$	$\frac{8-3\sqrt{15}}{72}$
$\frac{1}{2}+\frac{\sqrt{15}}{10}$	$\frac{29+6\sqrt{15}}{180}$	$\frac{8+3\sqrt{15}}{45}$	$\frac{29}{180}$
	$\frac{5}{18}$	$\frac{4}{9}$	$\frac{5}{18}$

(b) Gauss collocation (order 6)

$\frac{1}{2}-\frac{\sqrt{15}}{10}$	$\frac{5}{36}$	$\frac{2}{9}-\frac{\sqrt{15}}{15}$	$\frac{5}{36}-\frac{\sqrt{15}}{30}$
$\frac{1}{2}$	$\frac{5}{36}+\frac{\sqrt{15}}{24}$	$\frac{2}{9}$	$\frac{5}{36}-\frac{\sqrt{15}}{24}$
$\frac{1}{2}+\frac{\sqrt{15}}{10}$	$\frac{5}{36}+\frac{\sqrt{15}}{30}$	$\frac{2}{9}+\frac{\sqrt{15}}{15}$	$\frac{5}{36}$
	$\frac{5}{18}$	$\frac{4}{9}$	$\frac{5}{18}$

IRK-DG Method under Right Radau Quadrature

For this case, as discussed in the proposition after (2.40), the DG method is equivalent to the collocation method with the right Radau points as collocation points as well as the CG method under the right Radau quadrature. The resulting IRK method is straightforward: the matrix $\boldsymbol{A}$ is given by, for $1 \le i, j \le s$,

$$a_{i,j} = \tilde{l}_{R,j}(\xi_{R,i}) = \int_0^{\xi_{R,i}} l_{R,j}(\eta)d\eta.$$

The above is also a consequence of $\boldsymbol{M}_{RQ} = \boldsymbol{M}_{QR} = \boldsymbol{I}$. This IRK-DG scheme is called Radau IIA in the literature (e.g., Hairer & Wanner 1991).

Note that if the quadrature points are not of right Radau type (e.g., left Radau or Gauss type), then the corresponding collocation method is different from the DG method using such a quadrature.

IRK-DG Method under Left Radau Quadrature

For this case, with $f_{L,j} = f(\xi_{L,i}, u_{L,j})$, $1 \le j \le s$, Eqs. (2.19) and (2.20) provide a system of s equations for s unknowns $u_{L,i}$, $1 \le i \le s$. An elegant derivation of the corresponding IRK method using the left Radau quadrature can be found in LeSaint & Raviart (1974). Although not mentioned in the cited reference, as discussed below, the result is an IRK method identical to Radau IA.

4 Accuracy

The following conditions play a crucial role in the orders of accuracy of RK methods as well as the uniqueness of the Radau type schemes. Condition $C(\eta)$ and especially $D(\zeta)$ are typically not easy to grasp. Using the IRK construction in the previous section, these conditions for the IRK-DG methods are relatively simple to interpret and easy to prove. Condition $C(\eta)$ amounts to a degree of precision of $\eta - 1$ for certain quadratures, and $D(\zeta)$ relates to the projection of the polynomial r_j defined by (3.28) onto $\boldsymbol{P}_{\zeta-1}$. For more on these conditions applied to general IRK methods, see, e.g., Hairer & Wanner (1991).

With quadrature points ξ_i, Butcher tableau with stage levels $c_i = \xi_i$ (leftmost column), quadrature weights b_j at ξ_j (bottom row), and matrix $\boldsymbol{A} = \{a_{ij}\}$ (upper right), $1 \le i, j \le s$, the conditions are:

$$B(p): \quad \sum_{i=1}^{s} b_i c_i^{q-1} = \frac{1}{q} \qquad q = 1, \dots, p\ ;$$

$$C(\eta): \quad \sum_{j=1}^{s} a_{ij} c_j^{q-1} = \frac{c_i^q}{q} \qquad i = 1, \dots, s, \quad q = 1, \dots, \eta\ ;$$

$$D(\zeta): \quad \sum_{i=1}^{s} b_i c_i^{q-1} a_{ij} = \frac{b_j}{q}(1 - c_j^q) \qquad j = 1, \dots, s, \quad q = 1, \dots, \zeta\ .$$

Butcher's Theorem. If the coefficients b_i, c_i, and a_{ij} of an RK method satisfy $B(p)$, $C(\eta)$, $D(\zeta)$ with $p \le 2\eta + 2$ and $p \le \eta + \zeta + 1$, then the method is of order p.

In other words, if conditions $B(p)$, $C(\eta)$, $D(\zeta)$ hold for highest possible integer values of p, η, and ζ, then the method is of order $\mathrm{Min}(p, 2\eta + 2, \eta + \zeta + 1)$.

Condition $B(p)$

This condition means the quadrature has a degree of precision $p - 1$ or of order p, i.e., it is exact for any polynomial v of degree $p - 1$ or less:

$$\int_0^1 v(\xi) d\xi = \sum_{j=1}^{s} b_j v(\xi_j).$$

Concerning IRK-DG, for the Radau quadratures, condition $B(2s - 1)$ holds, and for Gauss, $B(2s)$.

Condition $C(\eta)$

This condition means for each i, $1 \le i \le s$, the following quadrature with weights a_{ij}, $1 \le j \le s$, has a degree of precision $\eta - 1$: for any v in $\boldsymbol{P}_{\eta-1}$,

$$\int_0^{c_i} v(\xi) d\xi = \sum_{j=1}^{s} a_{ij} v(\xi_j). \tag{4.1}$$

Indeed, with i and q fixed, by applying the quadrature rule of weights a_{ij} at quadrature points ξ_j, $1 \le j \le s$, we have the following approximation: $\int_0^{c_i} \xi^{q-1} d\xi \approx \sum_{j=1}^{s} a_{ij} \xi_j^{q-1}$. If the quadrature is exact, then

$$\sum_{j=1}^{s} a_{ij} \xi_j^{q-1} = \frac{c_i^q}{q}. \tag{4.2}$$

The monomials ξ^{q-1}, $q = 1, \dots, \eta$, form a basis for $\boldsymbol{P}_{\eta-1}$. Due to linearity, the fact that the above holds for $q = 1, \dots, \eta$ is equivalent to the fact that (4.1) holds for all v in $\boldsymbol{P}_{\eta-1}$, and the claim follows.

Condition $C(s)$ holds for the DG method under the right Radau quadrature,

Indeed, with such a quadrature, the DG method is equivalent to the right Radau collocation method as shown by the proposition before (2.41). Thus, for each i, $1 \le i \le s$, the quadrature formula

$$\int_0^{\xi_{R,i}} f_h(\eta)d\eta = \sum_{j=1}^{s} f_{R,j}\, \tilde{l}_{R,j}(\xi_{R,i}) = \sum_{j=1}^{s} a_{ij} f_{R,j} \tag{4.3}$$

is exact for any f_h in $\boldsymbol{P}_{s-1}$ and the above claim of $C(s)$ follows.

Condition $C(s-1)$ holds for an IRK-DG method under any quadrature of degree of precision $2s-2$ or higher. In other words, the degree of precision of (4.1) is reduced by 1, a consequence of r_j of degree $s-1$ approximating $\tilde{l}_j$ of degree s to one degree lower as discussed in (3.26)-(3.28).

To prove condition $C(s-1)$, with $1 \le q \le s-1$, set

$$v(\xi) = \xi^{q-1}. \tag{4.4}$$

Note that $v(\xi) = \sum_{j=1}^{s} \xi_j^{q-1} l_j(\xi)$ is of degree $\le s-2$ (in spite of each l_j being of degree $s-1$). Next,

$$\tilde{v}(\xi) = \int_0^{\xi} v(\tau)d\tau = \frac{\xi^q}{q} = \sum_{j=1}^{s} \xi_j^{q-1} \tilde{l}_j(\xi)$$

is of degree $q \le s-1$ (in spite of each $\tilde{l}_j$ being of degree s). Consequently, the s values of $\tilde{v}$ at the right Radau points, namely $\tilde{v}(\xi_{R,i})$, $i = 1, \dots, s$, determine a polynomial r identical to $\tilde{v}$**:**

$$r(\xi) = \tilde{v}(\xi) = \frac{\xi^q}{q}.$$

(Here, if $q = s$, i.e., $v(\xi) = \xi^{s-1}$, then r has degree $s-1$, $\tilde{v}$ has degree s, $r \ne \tilde{v}$, and the argument fails.) For each fixed i, by (3.26),

$$r(\xi_i) = \sum_{j=1}^{s} a_{ij} \xi_j^{q-1}.$$

The above two equations imply, since $c_i = \xi_i$, for $1 \le i \le s$, and $1 \le q \le s-1$

$$\sum_{j=1}^{s} a_{ij} c_j^{q-1} = \frac{c_i^q}{q}.$$

This completes the proof.

Condition $D(\zeta)$.

This condition relates to the projection of r_j onto $\boldsymbol{P}_{\zeta-1}$ as follows. For each fixed j, r_j defined by (3.27) is of degree $s-1$. If v is of degree $s-1$ or less, then vr_j is of degree $2s-2$ or less. Since the quadrature associated with ξ_i's has a degree of precision $2s-2$ or higher,

$$\int_0^1 v(\xi)\, r_j(\xi)d\xi = \sum_{i=1}^{s} b_i v(\xi_i) r_j(\xi_i) = \sum_{i=1}^{s} b_i v(\xi_i) a_{ij}, \tag{4.5}$$

where the last equality follows since $r_j(\xi_i) = a_{ij}$ by (3.28). Next, similar to (4.4), but with $1 \le q \le s$, set $v(\xi) = \xi^{q-1}$. Then v is of degree $s-1$ or less. Eq. (4.5) implies,

$$\left(r_j, \xi^{q-1}\right) = \int_0^1 \xi^{q-1}\, r_j(\xi)d\xi = \sum_{i=1}^{s} b_i \xi_i^{q-1} a_{ij}. \tag{4.6}$$

The above determines the projection of r_j onto $\boldsymbol{P}_{s-1}$ by using the quadrature associated with ξ_i's.

Thus, condition $D(\zeta)$ means for all j, the projection of r_j onto $\boldsymbol{P}_{\zeta-1}$ is given exactly by the quadrature associated with ξ_i's. We can now show the following.

Condition $D(s-1)$ holds for an IRK-DG method under any quadrature of degree of precision $2s-2$ or higher. The condition resulting in $D(s)$ will be discussed following the completion of this proof.

Indeed, the key to the proof is to replace r_j by $\tilde{l}_j$ in the left-hand side above. With $1 \le q \le s-1$, or $q-1 \le s-2$, we focus on the projection of r_j onto $\boldsymbol{P}_{s-2}$. By employing the s-point right Radau quadrature, and since $\tilde{l}_j - r_j$ vanishes at the right Radau points (r_j interpolates $\tilde{l}_j$ at the right Radau points),

$$\left(\tilde{l}_j - r_j, \xi^{q-1}\right) = 0. \tag{4.7}$$

That is, $\tilde{l}_j$ and r_j have the same projection onto $\boldsymbol{P}_{s-2}$:

$$\int_0^1 \xi^{q-1}\, r_j(\xi) d\xi = \int_0^1 \xi^{q-1}\, \tilde{l}_j(\xi) d\xi. \tag{4.8}$$

Concerning the right-hand side above, by integration by parts,

$$\int_0^1 \xi^{q-1}\, \tilde{l}_j(\xi) d\xi = \frac{1}{q}\left[\xi^q\, \tilde{l}_j\right]_0^1 - \frac{1}{q}\int_0^1 \xi^q\, l_j(\xi) d\xi. \tag{4.9}$$

For the last term above, since $l_j(\xi_i) = \delta_{ij}$, and $\xi_j = c_j$, by applying the quadrature,

$$\int_0^1 \xi^q\, l_j(\xi) d\xi = b_j c_j^q.$$

Substituting the above into (4.9), we obtain

$$\int_0^1 \xi^{q-1}\, \tilde{l}_j(\xi) d\xi = \frac{b_j}{q}(1 - c_j^q).$$

Finally, by (4.8), (4.6), and the above, for $1 \le q \le s-1$,

$$\sum\nolimits_{i=1}^{s} b_i c_i^{q-1} a_{ij} = \frac{b_j}{q}\left(1 - c_j^q\right). \tag{4.10}$$

This completes the proof.

Condition $D(s)$ holds for the DG method under the left Radau quadrature.

Indeed, we wish to show (4.10) for $1 \le q \le s$. To this end, since $q-1 \le s-1$, for the projection of r_j onto $\boldsymbol{P}_{s-1}$, consider $\left(r_j, \xi^{q-1}\right)$. We have, by using the quadrature, which is of left Radau type here,

$$\left(r_j, \xi^{q-1}\right) = \int_0^1 \xi^{q-1}\, r_j(\xi) d\xi = \sum\nolimits_{i=1}^{s} b_i c_i^{q-1} a_{ij}. \tag{4.11}$$

To prove (4.10) for $1 \le q \le s$, first, consider the case $j = 1$. Since $l_1 = l_{L,1}$, by (2.21), $l_1 = -g'/s^2$. Consequently, $\tilde{l}_1 = \text{constant} - g/s^2$. Next, since $\tilde{l}_1(0) = 0$, and $g(0) = 1$,

$$\tilde{l}_1 = \frac{1-g}{s^2}. \tag{4.12}$$

At the right Radau points, $g\left(\xi_{R,i}\right) = 0,\ i = 1, \dots, s$; therefore, $\tilde{l}_1\left(\xi_{R,i}\right) = 1/s^2$. Thus, r_1 defined by $\tilde{l}_1\left(\xi_{R,i}\right)$, $1 \le i \le s$, is a constant function: $r_1(\xi) = 1/s^2$. As a result, for $1 \le i \le s$,

$$a_{i1} = r_1(\xi_i) = \frac{1}{s^2} = b_1.$$

Consequently, for $1 \le q \le s$,

$$\sum\nolimits_{i=1}^{s} b_i c_i^{q-1} a_{i1} = b_1 \sum\nolimits_{i=1}^{s} b_i c_i^{q-1} = b_1 \int_0^1 \xi^{q-1} d\xi = \frac{b_1}{q}. \tag{4.13}$$

That is, (4.10) holds with $1 \le q \le s$ for $j = 1$.

For $j \ge 2$, again with $1 \le q \le s$, by applying integration by parts to $\left(\xi^{q-1}, r_j\right)$,

$$\int_0^1 \xi^{q-1}\, r_j(\xi) d\xi = \frac{1}{q}\left[\xi^q\, r_j\right]_0^1 - \frac{1}{q}\int_0^1 \xi^q\, r_j'(\xi) d\xi. \tag{4.14}$$

Since the quadrature points are the left Radau points, $r_j(1) = \tilde{l}_{L,j}(1) = b_{L,j} = b_j$. Thus,

$$\left[\xi^q\, r_j\right]_0^1 = b_j. \tag{4.15}$$

Next, note that $\tilde{l}_{L,j} - r_j$ is of degree s and vanishes at the right Radau points; therefore, $\tilde{l}_{L,j} - r_j = cg$ for some constant c. Since g' vanishes at all left Radau points except at $\xi = 0$, we have, for $2 \le i \le s$,

$$r_j'(\xi_{L,i}) = \tilde{l}_{L,j}'(\xi_{L,i}) = l_{L,j}(\xi_{L,i}) = \delta_{ij}.$$

By applying the left Radau quadrature to the last term of (4.14), the above implies, for $1 \le q \le s$,

$$\int_0^1 \xi^q\, r_j'(\xi) d\xi = \sum\nolimits_{i=1}^{s} b_{L,i}\xi_{L,i}^q r_j'(\xi_{L,i}) = \sum\nolimits_{i=1}^{s} b_{L,i}\xi_{L,i}^q \delta_{ij} = b_{L,j}\xi_{L,j}^q = b_j\xi_j^q. \tag{4.16}$$

Using (4.15) and (4.16), Eq. (4.14) implies

$$\int_0^1 \xi^{q-1}\, r_j(\xi) d\xi = \frac{b_j}{q} - \frac{b_j\xi_j^q}{q} = \frac{b_j}{q}\left(1 - \xi_j^q\right).$$

By (4.6) and the above, for $1 \le q \le s$,

$$\sum\nolimits_{i=1}^{s} b_i\xi_i^{q-1} a_{ij} = \frac{b_j}{s}\left(1 - \xi_j^q\right). \tag{4.17}$$

That is, (4.10) with $1 \le q \le s$ holds for $j \ge 2$. This, together with (4.13), completes the proof.

Conditions $B(p)$, $C(\eta)$, and $D(\zeta)$ for IRK-DG Method

The above argument shows that the following table of conditions holds for the IRK-DG method.

Table 4.1

Quadrature	IRK-DG method	$B(p)$	$C(\eta)$	$D(\zeta)$
Left Radau	Radau IA	$B(2s-1)$	$C(s-1)$	$D(s)$
Right Radau	Radau IIA	$B(2s-1)$	$C(s)$	$D(s-1)$
Gauss	DG-Gauss	$B(2s)$	$C(s-1)$	$D(s-1)$

By Butcher's theorem, the orders of accuracy are: for Radau IA,

$$\text{Min}(p, 2\eta+2, \eta+\zeta+1) = \text{Min}(2s-1, 2s, 2s) = 2s-1;$$

for Radau IIA,

$$\text{Min}(p, 2\eta+2, \eta+\zeta+1) = \text{Min}(2s-1, 2s+2, 2s) = 2s-1;$$

and, for DG with a quadrature of degree of precision $2s-2$ or higher as in our assumption ($p \ge 2s-1$),

$$\text{Min}(p, 2\eta+2, \eta+\zeta+1) = \text{Min}(p, 2s, 2s-1) = 2s-1.$$

That is, all IRK-DG methods with solution of degree $s-1$ are accurate to order $2s-1$.

Uniqueness of Matrix $\boldsymbol{A}$ by Condition $C(s)$ for IRK Method with Right Radau Quadrature

If c_i's are the right Radau points, $c_i = \xi_{R,i}$, and b_j's are the right Radau quadrature weights, $b_j = b_{R,j}$, $1 \le i, j \le s$, then condition $C(s)$ uniquely determines $\boldsymbol{A}$. Consequently, $C(s)$ implies $D(s-1)$.

Indeed, with $c_i = \xi_{R,i}$, let the corresponding Lagrange polynomials be $l_i = l_{R,i}$, $1 \le i \le s$, and set $\tilde{l}_j(\xi) = \int_0^\xi l_j(\eta) d\eta$. By (4.3), the matrix $\left\{\tilde{l}_j(c_i)\right\}_{i,j=1}^s$ satisfies condition $C(s)$.

Next, let $\left\{A_{ij}\right\}_{i,j=1}^s$ be a matrix satisfying condition $C(s)$. By (4.1), the following quadrature has a degree of precision $s-1$: for any v in $\boldsymbol{P}_{s-1}$,

$$\int_0^{c_i} v(\eta) d\eta = \sum\nolimits_{j=1}^{s} v(c_j) A_{ij}. \tag{4.18}$$

Uniqueness of $\boldsymbol{A}$ follows if we can show that $A_{ij} = \tilde{l}_j(c_i)$, $1 \le i, j \le s$.

To this end, with a fixed j, set $v = l_j$ in the above and, since $l_j(c_m) = \delta_{jm}$, we obtain

$$\int_0^{c_i} l_j(\eta)d\eta = \sum_{m=1}^{s} l_j(c_m)A_{im} = A_{ij}. \tag{4.19}$$

Next, by the definition of $\tilde{l}_j$, $\int_0^{c_i} l_j(\eta)d\eta = \tilde{l}_j(c_i)$. This fact and the above imply, for $1 \le i, m \le s$,

$$A_{ij} = \tilde{l}_j(c_i).$$

This completes the proof.

An IRK method using the right Radau quadrature is uniquely determined by condition $C(s)$. That is, such a method is identical to the IRK-DG scheme under the same quadrature as well as the IRK method for the right Radau collocation scheme. Consequently, condition $D(s-1)$ holds. The method is called Radau IIA in the literature (e.g., Hairer & Wanner 1991).

Uniqueness of Matrix $\boldsymbol{A}$ by Condition $D(s)$ for IRK Method with Left Radau Quadrature

If c_i's are the left Radau points, $c_i = \xi_{L,i}$, and b_j's are the corresponding quadrature weights, $b_j = b_{L,j}$, $1 \le i, j \le s$, then condition $D(s)$ uniquely determines $\boldsymbol{A}$. Consequently, $D(s)$ implies $C(s-1)$.

For the proof, with r_j defined by (3.27), using the left Radau quadrature, for $q \le s$,

$$\left(r_j, \xi^{q-1}\right) = \sum_{i=1}^{s} b_i c_i^{q-1} a_{ij} = \frac{b_j}{q}\left(1 - c_j^q\right).$$

Next, let $\{A_{i,j}\}$ be an $s \times s$ matrix that satisfy condition $D(s)$: for $1 \le j, q \le s$,

$$\sum_{i=1}^{s} b_i c_i^{q-1} A_{ij} = \frac{b_j}{q}\left(1 - c_j^q\right).$$

Let R_j be a polynomial of degree $s-1$ defined by $R_j(\xi_i) = A_{ij}$. Then, for a fixed j, by using the (left Radau) quadrature,

$$\left(R_j, \xi^{q-1}\right) = \sum_{i=1}^{s} b_i \xi_i^{q-1} A_{ij} = \frac{b_j}{q}\left(1 - c_j^q\right).$$

Since R_j and r_j are of degree $s-1$ and they have the same projection onto $\boldsymbol{P}_{s-1}$, $R_j = r_j$. Consequently, for $1 \le i, j \le s$, $R_j(\xi_i) = r_j(\xi_i)$, or

$$A_{ij} = a_{ij}.$$

This completes the proof.

Therefore, an IRK method using the left Radau quadrature is uniquely determined by condition $D(s)$. Such a method is thus identical to the IRK-DG scheme under the left Radau quadrature and, as a result, condition $C(s-1)$ holds. The method is called Radau IA in the literature (e.g., Hairer & Wanner 1991).

5 Numerical Examples of DG Solutions

Two simple examples show the behavior of the DG solutions u_h and U.

For the first example, the ODE on $[0, 1]$ is given by

$$u'(x) = f(x) = \pi \cos(\pi x + \frac{\pi}{6}), \qquad u(0) = \frac{1}{2}.$$

With step size $h = 1$, we wish to obtain the DG solutions u_h and U using the left Radau, Gauss, and right Radau quadratures for each of the two cases $k = 1$ and $k = 2$. The exact solution is obvious:

$$u_{\text{exact}}(x) = \sin\left(\pi x + \frac{\pi}{6}\right).$$

The DG solution $u_{n+1} = u_h(1) = U(1)$ reduces to the solution by the quadrature formula as shown below. Consequently, the Gauss quadrature produces a result accurate to one order higher than the two Radau quadratures. This gain in accuracy, however, does not hold in the second example.

For the quadratures employed, the projection of f reduces to interpolation, i.e., with quadrature points ξ_i, $1 \le i \le k+1$, f_h is defined by $f(\xi_i)$: $f_h = \mathcal{P}_k(f) = \sum_{i=1}^{k+1} f(\xi_i) l_i$. The solution U is given by (2.34):

$$U(\xi) = \frac{1}{2} + \int_0^{\xi} f_h(\eta) d\eta = \frac{1}{2} + \sum_{i=1}^{k+1} f(\xi_i) \int_0^{\xi} l_i(\eta) d\eta.$$

At the end of the step,

$$U(1) = \frac{1}{2} + \int_0^{1} f_h(\eta) d\eta = \frac{1}{2} + \sum_{i=1}^{k+1} b_i f(\xi_i).$$

That is, the DG solution U reduces to the quadrature formula. As for u_h, it is defined by $U(\xi_{R,i})$ at the right Radau points $\xi_{R,i}$, $1 \le i \le k+1$.

Fig. 5.1 shows, on $[0, 1]$, the graphs of the exact f (thin red curve) and, for the case $k = 1$, the linear f_h (thick blue line) defined by the values at the two quadrature points (red square dots) of type (a) left Radau, (b) Gauss, and (c) right Radau.

Fig. 5.2 shows the graphs of the exact solution u_{exact} (thin red curve) and, for $k = 1$, the quadratic DG solution U (thick blue curve) as well as the linear DG solution u_h (dot-dashed green curve); again, the quadrature points are of type (a) left Radau, (b) Gauss, and (c) right Radau. Here, each continuous curve is the integral of the corresponding counterpart in Fig. 5.1 with $u(0) = 1/2$. For $1 \le i \le k+1$, the solutions $u_{n,i}$ at the quadrature points by the IRK-DG method are shown as the large green square dots on the line u_h. Note that the solution at $\xi = 1$ in (b) is most accurate, a fact consistent with the Gauss quadrature being more accurate by one order compared with the Radau quadratures.

Fig. 5.3 is analogous to Fig. 5.1 but with $k = 2$, and the same is true for Fig. 5.4 relative to Fig. 5.2.

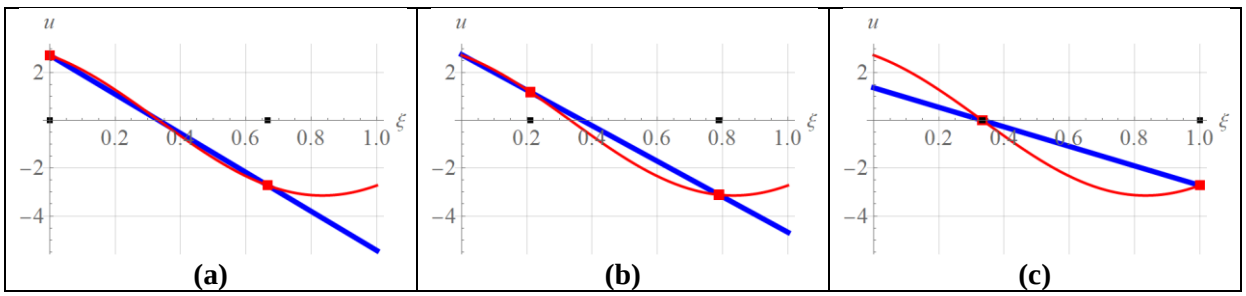

Fig. 5.1 The graphs of f_{exact} (red curve) and, for $k = 1$, the linear f_h (thick blue line) defined by the values at the two quadrature points (red square dots) of type **(a)** left Radau, **(b)** Gauss, and **(c)** right Radau.

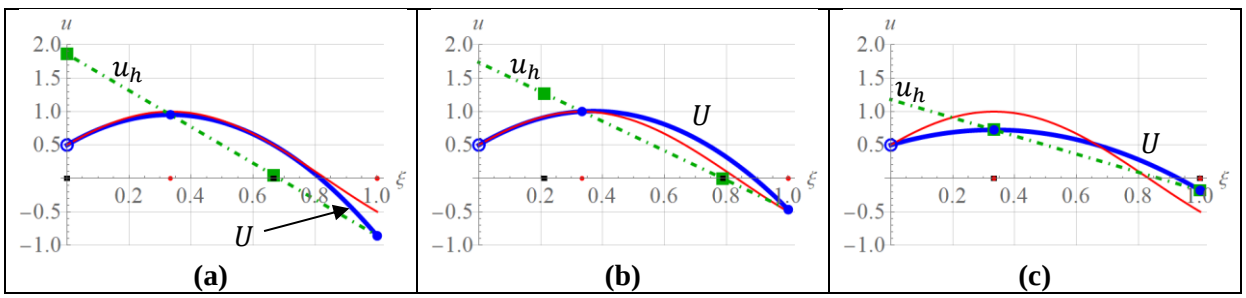

Fig. 5.2 The graphs of u_{exact} (red curve) and, for $k = 1$, the quadratic U (thick blue curve) and the linear u_h (dot-dashed green line); the quadrature points are of type: **(a)** left Radau, **(b)** Gauss, and **(c)** right Radau.

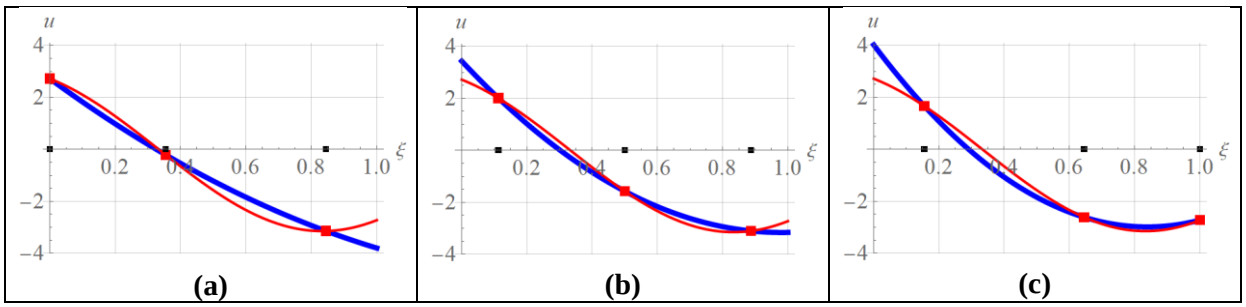

Fig. 5.3 The graphs of f_{exact} (red curve) and, for $k = 2$, the quadratic f_h (thick blue curve) defined by the values at three quadrature points (red square dots) of type **(a)** left Radau, **(b)** Gauss, and **(c)** right Radau.

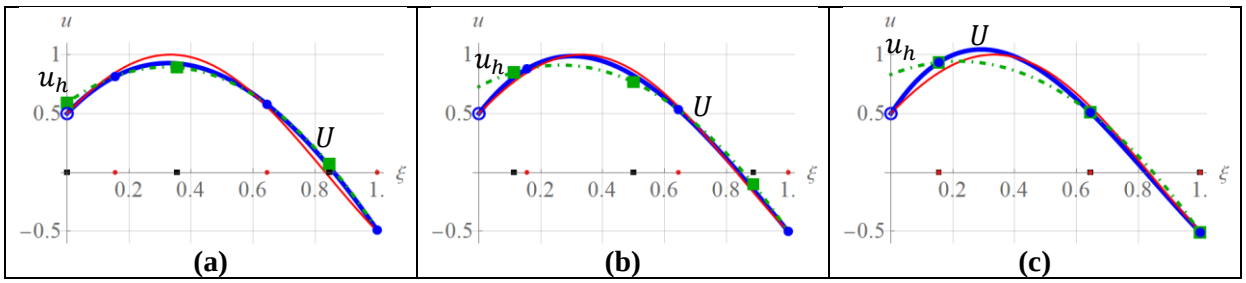

Fig. 5.4 The graphs of u_{exact} (red curve) and, for $k = 2$, the cubic U (thick blue curve), and quadratic u_h (dot-dashed green curve); the quadrature points are of type **(a)** left Radau, **(b)** Gauss, and **(c)** right Radau.

For the second and final example, the ODE on $[0, 1]$ is $u' = \lambda u$. We employ two different values for λ, $2\pi i/3$ and $\pi i/3$, which is equivalent to halving the step size; here, i is the imaginary number. The initial condition is $u(0) = 1$. The exact solution is $u_{\text{exact}}(\xi) = e^{\lambda \xi}$. We wish to obtain the DG solutions u_h and U with $h = 1$ for both $k = 1$ and $k = 2$.

For this problem, if v is of degree k, then $u_h' v$, $u_h v'$, and $u_h v$ are of degree $2k$ or less. Therefore, provided the quadrature has a degree of precision $2k$ or higher, by either the weak form (2.2) or the strong form (2.3), the DG solution is independent of the quadrature employed.

Fig. 5.5 shows the graphs of u_{exact} (red dashed curve) and the DG solutions u_h (dot-dashed green line) and U (continuous blue curve) for the case $k = 1$ where λ equals (a) $2\pi i/3$ and (b) $\pi i/3$.

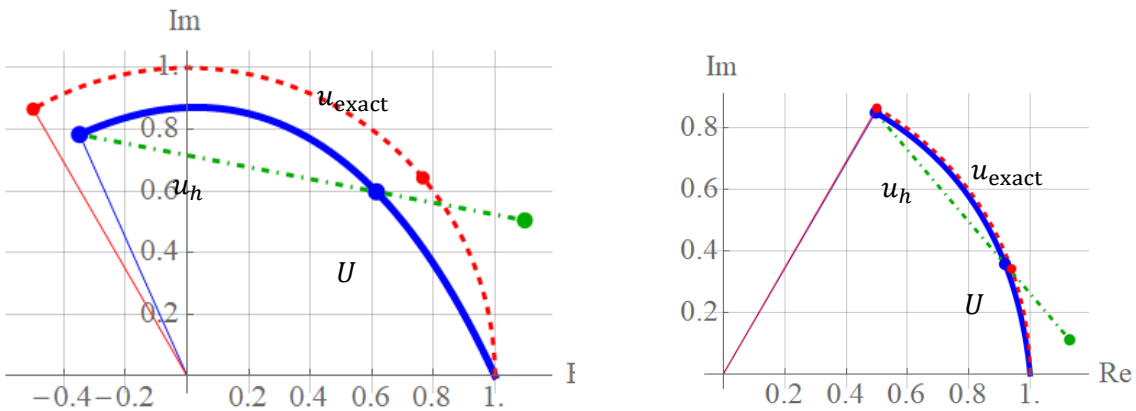

Fig. 5.5 The graphs of u_{exact} (red dashed curve) and the DG solutions u_h (dot-dashed green line) and U (continuous blue curve) for the case $k = 1$ where **(a)** $\lambda = 2\pi i/3$ and **(b)** $\lambda = \pi i/3$.

Fig. 5.6 is analogous to Fig. 5.5 but with $k = 2$.

Note the significant improvement in accuracy by halving the step size (λ from $2\pi i/3$ to $\pi i/3$) or by increasing the degree of approximation (k from 1 to 2).

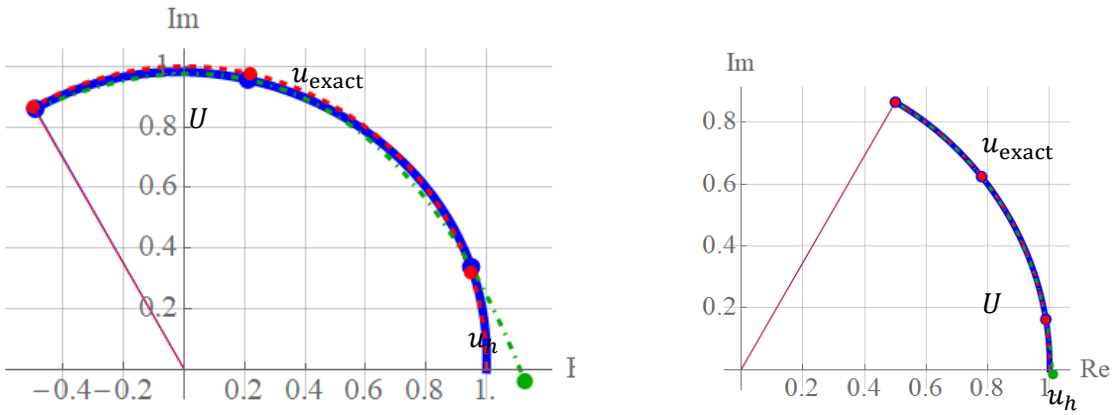

(a) **(b)**

Fig. 5.6 The graphs of u_{exact} (red dashed curve) and the DG solutions u_h (dot-dashed green line) and U (continuous blue curve) for the case $k = 2$ where **(a)** $\lambda = 2\pi i/3$ and **(b)** $\lambda = \pi i/3$.

The error in the DG solution $u_h(1)$ is

$$\text{Er} = |u_{\text{exact}}(1) - u_h(1)|.$$

In the piecewise linear case of Fig. 5.5, for $\lambda = 2\pi i/3$, the error is $\text{Er}_1 \approx 0.1720$; for $\lambda = \pi i/3$, $\text{Er}_2 \approx 0.01520$ resulting in $\text{Er}_1/\text{Er}_2 \approx 11.3$. The next halving of the step size ($\lambda = \pi i/6$) results in $\text{Er}_2/\text{Er}_3 \approx 14.9$ and then 15.7 approaching a ratio of $16 = 2^4$. Thus, the error reduction is consistent with the fact that the piecewise linear DG method for ODE is third-order accurate. Similarly, the piecewise parabolic DG solution is fifth-order accurate. We omit the details.

6 Conclusions and Discussion

In summary, we studied the numerical solutions for ODE by the DG method from a perspective different from those in the literature. Our focus was on constructing the solution by first deriving the DG method in differential form. The derivation is made possible by a polynomial called the correction function, which approximates the jump at the beginning of each step. The correction function facilitates the construction of the IRK-DG schemes under different quadratures. The IRK-DG construction in turn clarifies the meaning and facilitates the proofs of various $B(p)$, $C(\eta)$, and $D(\zeta)$ conditions, which play a crucial role in the order of accuracy of the schemes as well as the uniqueness of the Radau type methods. Numerical examples were provided. In all, the correction function plays a central role and clarifies the relations among the DG and related schemes.

The current approach can potentially be employed to simplify the time discretization of the space-time DG methods (e.g., Johnson et al. 1984, Van der Vegt & Van der Ven 2002, Murman et al. 2016). Iterative procedures amenable to modern supercomputers for the IRK as well as other high-order time stepping methods are currently an active area of research (Wang et al. 2013, Slotnick et al. 2014).

Acknowledgements. The author was supported by the Transformational Tools and Technologies Project of NASA. He also wishes to thank Dr. Dimitri Mavriplis for several interesting discussions on DG methods applied to time stepping and Dr. Seth Spiegel for his thorough review.

References

[1] S. Adjerid, K.D. Devine, and J.E. Flaherty and L. Krivodonova, A posteriori error estimation for discontinuous Galerkin solutions of hyperbolic problems, Comput Methods Appl Mech Eng, 191 (2002), pp. 1097-1112.

[2] J.H. Argyris and D.W. Scharpf, Finite elements in time and space, Aer. J. Royal Aer. Soc., 73, 1041-1044 (1969).

[3] O. Axelsson, A class of A-stable Methods, Nordisk Tidskr. Informationbehandling (BIT), v. 9, 1969, pp. 185-199.

[4] M. Baccouch, Analysis of a posteriori error estimates of the discontinuous Galerkin method for nonlinear ordinary differential equations, Applied Numerical Mathematics 106 (2016) 129–153.

[5] M. Borri and C.L. Bottasso, A general framework for interpreting time finite element formulations, Comput. Mech., 13, 133-142 (1993).

[6] C.L. Bottasso, A new look at finite elements in time: a variational interpretation of Runge-Kutta methods, Applied Numerical Mathematics, 25, 355-368 (1997).

[7] B. Cockburn, G. Karniadakis, and C.-W. Shu, Discontinuous Galerkin methods: Theory, Computation, and Applications, Springer (2000).

[8] G. J. Cooper, Interpolation and quadrature methods for ordinary differential equations, Math. Comp., v. 22, 1968, pp. 69-76.

[9] M. Delfour, W. Hager, and F. Trochu, Discontinuous Galerkin methods for ordinary differential equations, Math. Comp., v. 36, 1981, pp. 455-473.

[10] B.L. Ehle, A-Stable Methods and Padé Approximations to the Exponential, SIAM Journal on Mathematical Analysis, v. 4, 1973, pp. 671-680.

[11] D. Estep and A. Stuart, The dynamical behavior of the discontinuous Galerkin method and related difference schemes, Math. Comput., 71, 1075-1103 (2001).

[12] K. Eriksson, D. Estep, P. Hansbo, and C. Johnson, Computational Differential Equations, Cambridge University Press (1996) or https://www.csc.kth.se/~jjan/private/cde.pdf (2009)

[13] I. Fried, Finite element analysis of time dependent phenomena, AIAA J., 7, 1170-1173 (1969).

[14] A. Fortina and D. Yakoubi, An adaptive discontinuous Galerkin method for very stiff systems of ordinary differential equations, Appl. Math. Comput, v. 358, 2019, pp. 330-347.

[15] E. Hairer, S. P. Norsett, and G. Wanner, Solving ordinary differential equations I, 2nd edition, Springer-Verlag (1993).

[16] E. Hairer and G. Wanner, Solving ordinary differential equations II, Springer-Verlag (1991).

[17] F.B. Hildebrand, Introduction to Numerical Analysis, Dover (1987).

[18] B. Hulme, Discrete Galerkin and related one-step methods for ordinary differential equations, Math. Comp., v. 26, 1972, pp. 881-891.

[19] Thomas J.R. Hughes, The finite element method, Dover Publications (2012).

[20] H.T. Huynh, A flux reconstruction approach to high-order schemes including discontinuous Galerkin methods, 18th AIAA-CFD Conference, AIAA paper 2007-4079.

[21] H.T. Huynh (2009a), A Reconstruction Approach to High-Order Schemes Including Discontinuous Galerkin for Diffusion, AIAA Paper 2009-403.

[22] H.T. Huynh (2009b), Collocation and Galerkin Time-Stepping Methods, AIAA Paper 2009-4323.

[23] H.T. Huynh, On Formulations of Discontinuous Galerkin and Related Methods for Conservation Laws, NASA/TM—2014-218135.

[24] H.T. Huynh, Z.J. Wang, P.E. Vincent, High-order methods for computational fluid dynamics: a brief review of compact differential formulations on unstructured grids. Comput. Fluids 98, 209–220 (2014).

[25] C. Johnson, Numerical Solution of Partial Differential Equations by the Finite Element method, Dover Publications (2012).

[26] C. Johnson, U. Nävert, and J. Pikäranta, Finite element methods for linear hyperbolic problems, Comput. Methods Appl. Mech. Eng., v. 45, 1984, pp. 285-312.

[27] J.D. Lambert, Numerical methods for ordinary differential systems, John Wiley and Sons (1991).

[28] P. LeSaint and P.A. Raviart, On the finite element method for solving the neutron transport equation, in C. de Boor, editor, Mathematical aspects of finite elements in partial differential equations, Academic Press (1974), pp. 89-145.

[29] S.M. Murman, L. Diosady, A. Garai, and M. Ceze, A Space-Time Discontinuous-Galerkin Approach for Separated Flows, AIAA Paper 2016-1059.
[30] W.H. Reed and T.R. Hill, Triangular mesh methods for the neutron transport equation, Tech. Report LA-UR-73-479, Los Alamos Scientific Laboratory, 1973.
[31] J. Slotnick, et al., CFD Vision 2030 Study: A Path to Revolutionary Computational Aerosciences, NASA/CR–2014-218178.
[32] S.C. Spiegel, M.R. Borghi and D.A. Yoder, Simulations of a Single-Injector Cooling Flow Using the High-Order Flux Reconstruction Method, AIAA Paper AIAA 2022-1813.
[33] W.S. Tang and Y.J. Sun, Time finite element methods: A unified framework for numerical discretizations of odes. Appl. Math. Comput. 2012, 219, 2158–2180.
[34] J.J.W. van der Vegt and H. van der Ven "Space-time discontinuous Galerkin finite element method with dynamic grid motion for inviscid compressible flows, Part I. General formulation", J. Comput. Phys., 182 (2002) 546-585.
[35] Wang, Z.J., et al.: High-order CFD methods: current status and perspective. Int. J. Numer. Meth. Fluids 72(8), 811–845 (2013).
[36] K. Wright, "Some relationship between implicit Runge-Kutta, Collocation and Lanczos τ-methods, and their stability properties", BIT, v. 10, 1970.
[37] Y. Xing, M. Qin, J. Guo, A Time Finite Element Method Based on the Differential Quadrature Rule and Hamilton's Variational Principle. Applied Sciences. 2017; 7(2):138.
[38] S. Zhao and G.W. Wei, A unified discontinuous Galerkin framework for time Integration, Mathematical Methods in the Applied Sciences, v. 37(7), 2014.